frontiers | Frontiers in Marine Science

TYPE Original Research
PUBLISHED 30 March 2023
DOI 10.3389/fmars.2023.1150488

OPEN ACCESS

EDITED BY
Şükrü Beşiktepe,
Dokuz Eylül University, Türkiye

REVIEWED BY
Hazem Nagy,
Alexandria University, Egypt
William Llovel,
UMR6523 Laboratoire d'Oceanographie Physique et Spatiale (LOPS), France

*CORRESPONDENCE
Matteo Meli
matteo.meli7@unibo.it

SPECIALTY SECTION
This article was submitted to Physical Oceanography, a section of the journal Frontiers in Marine Science

RECEIVED 24 January 2023
ACCEPTED 15 March 2023
PUBLISHED 30 March 2023

CITATION
Meli M, Camargo CML, Olivieri M, Slangen ABA and Romagnoli C (2023) Sea-level trend variability in the Mediterranean during the 1993–2019 period. *Front. Mar. Sci.* 10:1150488. doi: 10.3389/fmars.2023.1150488

Sea-level trend variability in the Mediterranean during the 1993–2019 period

Matteo Meli [1*], Carolina M. L. Camargo [2,3], Marco Olivieri [4], Aimée B. A. Slangen [2] and Claudia Romagnoli [1]

[1]Department of Biological, Geological and Environmental Sciences, University of Bologna, Bologna, Italy, [2]Department of Estuarine and Delta Systems, Royal Netherlands Institute for Sea Research (NIOZ), Yerseke, Netherlands, [3]Department of Geoscience and Remote Sensing, Delft University of Technology, Delft, Netherlands, [4]Istituto Nazionale di Geofisica e Vulcanologia (INGV), Sezione di Bologna, Bologna, Italy

Sea-level change is one of the most concerning climate change and global warming consequences, especially impacting coastal societies and environments. The spatial and temporal variability of sea level is neither linear nor globally uniform, especially in semi-enclosed basins such as the Mediterranean Sea, which is considered a hot spot regarding expected impacts related to climate change. This study investigates sea-level trends and their variability over the Mediterranean Sea from 1993 to 2019. We use gridded sea-level anomaly products from satellite altimetry for the total observed sea level, whereas ocean temperature and salinity profiles from reanalysis were used to compute the thermosteric and halosteric effects, respectively, and the steric component of the sea level. We perform a statistical change point detection to assess the spatial and temporal significance of each trend change. The linear trend provides a clear indication of the non-steric effects as the dominant drivers over the entire period at the Mediterranean Sea scale, except for the Levantine and Aegean sub-basins, where the steric component explains the majority of the sea-level trend. The main changes in sea-level trends are detected around 1997, 2006, 2010, and 2016, associated with Northern Ionian Gyre reversal episodes, which changed the thermohaline properties and water mass redistribution over the sub-basins.

KEYWORDS

Mediterranean Sea, sea-level change, satellite altimetry, steric component, thermosteric and halosteric effects, trend variability, sub-basins scale variability

1 Introduction

Sea-level change observations have been considered one of the key aspects of climate change reconstruction over the last few decades because of their interconnection with all other climate indicators, such as atmospheric temperature. Therefore, global mean sea-level assessment has been one of the main objectives of different studies in the past few decades (Fox-Kemper et al., 2021).

Global mean sea-level change is determined by mass addition, driven by continental ice melting and changes in land water storage, and the steric effect that is driven by changes in water column density induced by salinity (negligible at the global scale) and thermal fluctuations (Levitus et al., 2012; Fox-Kemper et al., 2021). However, sea-level change at the global scale is far from uniform, and on a regional to local scale it can vary greatly from global mean rates (e.g., Stammer et al., 2013; Jevrejeva et al., 2014; Slangen et al., 2014). For instance, sea-level trends in the Mediterranean differ from global mean sea-level trends, mainly because of its semi-enclosed conditions (Pinardi et al., 2014), and can even differ from the values observed in the nearby Atlantic Ocean (Tsimplis and Baker, 2000). Sea level in the Mediterranean has changed with a rate of 2.5 ± 0.4 mm/yr from 1993 to 2017 (Mohamed et al., 2019a), compared to a global mean rate of 3.2 ± 0.4 mm/yr for a similar period (Fox-Kemper et al., 2021). Additionally, within the Mediterranean, sea-level trends can differ from the basin mean (Bonaduce et al., 2016; Mohamed et al., 2019a; Calafat et al., 2022) due to non-linear local oceanographic processes (Vera et al., 2009).

Because of the many low-lying densely inhabited coastal areas, the Mediterranean Sea has been classified as one of the most susceptible climate change zones worldwide (Giorgi, 2006). Sea-level rise and related future projections (IPCC, 2021) may significantly impact coastal populations and activities, strengthening climate-related concerns and prompting a better understanding of processes from a global to a regional and local scale. Furthermore, the low elevation may significantly exacerbate sea-level rise at several coastal locations throughout the Mediterranean Sea, due to the local vertical land motion processes. These are caused by a combination of natural factors such as the compaction of alluvial sediments and volcanic-tectonic activity, as well as anthropogenic factors including the extraction of underground fluids (Gambolati and Teatini, 1998; Syvitski et al., 2009). These processes can cause land subsidence and amplify the effects of rising sea levels in these regions (García et al., 2007; Wöppelmann and Marcos, 2012; Mohamed et al., 2019b). Thus, there is a need to understand sea level change at the scale of the Mediterranean Sea.

This study focuses on sea-level variations in the Mediterranean Sea region (Figure 1A) to elucidate the large variability that occurred at both regional and sub-basin scales over the period 1993-2019. Most of the previous studies of the Mediterranean focus on trends either at the basin scale or in a specific region. Hence, there is a gap in understanding the changes in sea level variability over the Mediterranean at a sub-basin scale, likely driven by internal processes within the domain and masked by averaging at larger scales. In this framework, this study analyzes the main variability of sea-level trends observed from altimetry (total sea level) and the related contributions of changes in water temperature (thermosteric effect) and salinity (halosteric effect), which together account for the steric component across the Mediterranean Sea and its sub-basins. The significance of the variability observed in sea-level trends is then discussed at different spatiotemporal scales.

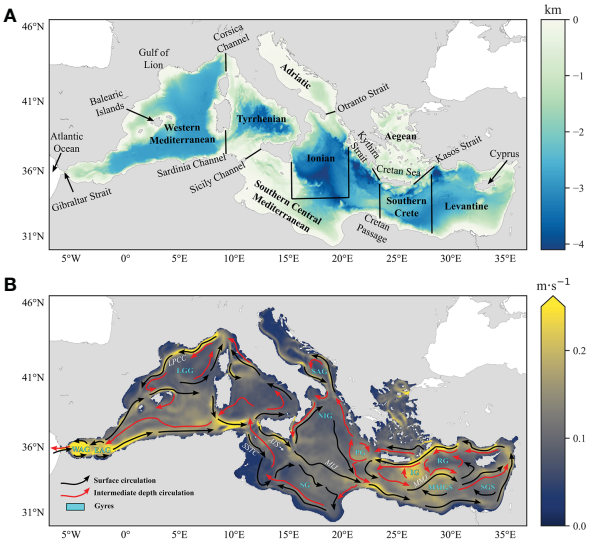

FIGURE 1
(A) Bathymetry of the Mediterranean Sea with regionalization of sub-basins (bold) and related borders. **(B)** Schematic representation of the surface (black arrows) and intermediate depth (red arrows) circulation in the Mediterranean Sea, superimposed on the map of 1993-2019 time-mean current velocities at 15 m depth. Both the bathymetry and current velocities are computed from the Mediterranean Sea Physics Reanalysis dataset (MEDSEA_MULTIYEAR_PHY_006_004). The labels of currents are in italics white, while gyres are in bold cyan. Acronyms: AIS, Atlantic Ionian Stream; AMC, Asia Minor Current; EAG, Eastern Alboran Gyre; EIC, Eastern Ionian Current; IG, Ierapetra Gyre; LGG, Gulf of Lion Gyre; LPCC, Liguro-Provencal-Catalan Current; MIJ, Mid-Ionian Jet; MMGS, Mersa Matruh Gyre System; MMJ, Mid-Mediterranean Jet; NIG, Northern Ionian Gyre; PG, Pelops Gyre; RG, Rhodes Gyre; SAG, Southern Adriatic Gyre; SG, Sirte Gyre; SGS; Shikmona Gyre System; SSTC, Sicily Strait Tunisian Current; WAG, Western Alboran Gyre.

1.1 General settings of the Mediterranean Sea

The Mediterranean Sea is a semi-enclosed, mid-latitude sea connected to the North Atlantic Ocean by the Gibraltar Strait (Figure 1A), where the exchange of water, heat, and salt occurs (Pinardi et al., 2015). The bathymetry of the basin (Figure 1A) varies significantly around the 1500 m average, ranging from a few tens of meters of depth (e.g., Northern Adriatic and Southern Central Mediterranean) to more than 4000 m depth (Tyrrhenian and Ionian) (Miramontes et al., 2022 and references therein).

The Mediterranean Sea can be divided into different sub-basins as (from west to east) the Western Mediterranean, Tyrrhenian, Ionian, Southern Central Mediterranean, Southern Crete, Levantine, and two marginal seas, Adriatic and Aegean (Figure 1A). The Western Mediterranean is connected from the Tyrrhenian by the Sardinia and Corsica channels, while the Tyrrhenian is connected from the Southern Central Mediterranean by the Sicily Channel (Figure 1A). Furthermore, the Southern Central Mediterranean is connected towards the east to the Southern Crete through the Cretan Passage (Figure 1A), whereas the connection/division with the Ionian is not purely based

on straits or passages but following variations in local bathymetry and oceanographic processes. Therefore, the latter can also be defined as a separation criterion in the case of Southern Crete and Levantine (Figure 1A). Finally, the Adriatic is connected to the Ionian by the Otranto Strait, whereas the Aegean is connected from the rest by the Kythira and Kasos straits (Figure 1A). Furthermore, to avoid confusion among the terms used in this study, we also define WMed and EMed as the macro-portions of the Mediterranean west and east of the Sicily Channel, respectively.

The Mediterranean receives ocean water from the Atlantic Ocean to compensate for a persistent surface water loss, mainly driven by evaporation (owing to the increase in sea surface temperature) and a persistent freshwater deficit (Romanou et al., 2010; Pastor et al., 2018), leading to basin-wide salinification (Grodsky et al., 2019). Excess evaporation over precipitation, especially in the EMed, forms high-salinity waters that drive and maintain the thermohaline circulation in the Mediterranean Sea through a large salinity contrast that forms between the Levantine waters and the inflowing waters at Gibraltar (Robinson et al., 2001), which contrasts with the thermohaline circulation outside the Mediterranean, dominated by divergences in heat content.

Deep-water masses are distinct between the WMed and EMed because of the occurrence of the Sicily Channel sill (Figure 1A). The WMed and EMed deep waters are formed in the Gulf of Lion (Figure 1A) and the Adriatic, respectively. Deep waters can also form in the Rhodes Gyre (RG, Figure 1B), namely the Levantine Intermediate Water (LIW; see Pinardi et al., 2015 and references therein). The key event for EMed circulation, linked to a yet not fully understood chain of oceanic, hydrological, and atmospheric interactions, was the migration of dense water formation from the Adriatic to the southern Aegean that occurred from the late eighties to the early nineties (Roether et al., 1996; Roether et al., 2014). This shift is known as the Eastern Mediterranean Transient (EMT; Roether et al., 1996; Malanotte-Rizzoli et al., 1999; Theocharis et al., 1999). It was a prolonged stepped process that culminated in 1997 with the so-called Northern Ionian Reversal phenomenon (Pinardi et al., 2015), that is, the shift of the Northern Ionian Gyre (NIG, Figure 1B) from the anticyclonic circulation mode to cyclonic circulation (Civitarese et al., 2010). This phenomenon has been reported multiple times over the last decades (Malanotte-Rizzoli et al., 1997; Pinardi et al., 1997; Malanotte-Rizzoli et al., 1999; Larnicol et al., 2002; Borzelli et al., 2009; Gačić et al., 2010; Gačić et al., 2011; Poulain et al., 2012; Menna et al., 2019; von Schuckmann et al., 2019), with the surface circulation oscillating from cyclonic to anticyclonic around 1987, 2006 and 2017 and vice-versa around 1997 and 2011.

This suggests that circulation reversal is a recurrent phenomenon that occurs on a quasi-decadal time scale in the EMed (or Ionian Sea region). However, there is a lack of consensus regarding the causes of the upper layer circulation pattern changes in the Ionian (see also Chiggiato et al., 2023). Some studies attributed it to internally driven processes (Pisacane et al., 2006; Borzelli et al., 2009; Gačić et al., 2010; Gačić et al., 2011; Gačić et al., 2014; Theocharis et al., 2014; Reale et al., 2016; Reale et al., 2017; Grodsky et al., 2019), while others indicated wind forcing as a possible mechanism (Korres et al., 2000; Demirov and Pinardi, 2002; Nagy et al., 2019). Regardless of the drivers, reversal events strongly impact the formation and distribution of water masses and influence local thermohaline properties throughout the Mediterranean sub-basins (von Schuckmann et al., 2019).

1.2 The ocean circulation in the Mediterranean Sea

Circulation in the Mediterranean (see Pinardi et al., 2015 for an extensive review) reflects its complexity, in which the northern regions are mainly characterized by cyclonic gyres, whereas anticyclonic gyres and eddy-dominated flow fields are predominant in the southern regions (Figure 1B), except for the northern Ionian Sea (Pinardi et al., 2015). Two types of circulation cells co-exist: a basinwide thermohaline circulation, driven mainly by the east-west salinity contrast between the Atlantic Water (AW) and the LIW, which is mainly limited to the surface and intermediate layers, and a deep circulation controlled by the north-south temperature gradient, where the driving mechanisms are winter air-sea heat losses and vertical convection (Gačić et al., 2014). Generally, the Mediterranean Sea is characterized by high salinity, temperature, and density, where net evaporation exceeds precipitation (Tanhua et al., 2013). This drives an anti-estuarine circulation at the Strait of Gibraltar (Figure 1A), where the incoming AW moves mainly eastward (Figure 1B) in the upper 50–100 m layer (Pinardi et al., 2015), overlying the LIW. As the AW moves east, it transforms into a warmer and saltier water mass due to wind-induced evaporation, in the Levantine (Lascaratos et al., 1993).

The circulation of the Mediterranean Sea is composed of several currents and gyres, as detailed in this paragraph (Figure 1B). The AW enters the WMed at Gibraltar, it meanders around the two anticyclonic western and eastern Alboran gyres (WAG and EAG; Heburn and La Violette, 1990) and then separates into two distinct currents, the first mainly flows towards the east (Millot, 1985; Ayoub et al., 1998) while the second flows northward towards the Balearic Islands and then towards east, along the southern boundary of the Gulf of Lion gyre (LGG; Madec et al., 1991; Pinardi et al., 2006). Simultaneously, the northern border of the cyclonic LGG is intensified by the Liguro–Provencal–Catalan Current (LPCC; Pinardi et al., 2006), which flows back to the Balearic Islands towards the southwest. In the Sardinia Channel, the different current merges and then split further into three branches (Beranger et al., 2004; Pinardi et al., 2006): one flowing towards the Tyrrhenian, whereas the other two branches enter the Sicily Channel, hence the EMed, forming the Atlantic Ionian Stream (AIS; Robinson et al., 1999) and Sicily Strait Tunisian Current (SSTC; Lermusiaux and Robinson, 2001; Onken et al., 2003).

In the central EMed, the SSTC flows along the southern coast of the south-central Mediterranean sub-basin, turning first northward and then eastward around the anticyclonic Sirte Gyre (SG; Pinardi et al., 2006). The most prominent oceanographic feature in the Ionian is represented by the NIG, which is characterized by a quasi-decadal reversal of the vorticity, from cyclonic to anticyclonic and vice-versa (see Section 1.1), capable of strongly impacting the

circulation at the sub-basin scale and beyond, especially by influencing the AW path by shifting the AIS position (Malanotte-Rizzoli et al., 1997; Menna et al., 2019). During the cyclonic state, the AIS is mainly prolonged toward the east, conveying AW directly to the Cretan passage through the shortest route by an intense current defined as Mid-Ionian Jet (MIJ; Robinson et al., 2001; Gačić et al., 2011; Bessières et al., 2013; Gačić et al., 2014). During anticyclonic phases, the AIS is primarily deflected towards north-east, meandering the northern Ionian and partially entering the Adriatic (Vilibić et al., 2012) and the Southern Adriatic Gyre (SAG; Artegiani et al., 1997) *via* the Otranto Strait, and then flowing south towards the Levantine, flanking the Pelops Gyre (PG; Robinson et al., 1992). In this configuration, the AW flows towards the Levantine are greatly reduced owing to the weakening of the MIJ (Gačić et al., 2011), whereas the thermohaline properties of the eastern EMed changes due to the longer path of the AW to reach the Cretan Passage (Gačić et al., 2014).

Once the AIS reaches the eastern EMed, passing through the Cretan Passage, it forms a broad current which flows along the North African coasts; part of it, branches the Mid-Mediterranean Jet (MMJ; Golnaraghi and Robinson, 1994). The MMJ is represented by a free open ocean jet meandering first between the Ierapetra Gyre (IG; Robinson et al., 1991), the Rhodes Gyre (RG; Milliff and Robinson, 1992), and the Mersa Matruh Gyre System (MMGS), then partially between Cyprus (Figure 1A) and the Shikmona Gyre System (SGS; Hecht et al., 1988).

As stated above, the Levantine represents the LIW area of formation, primarily in the RG, which is representative of the intermediate depth circulation in the Mediterranean Sea (Figure 1B) as the average currents between 200 and 300 m depth (Pinardi et al., 2015), flowing in the opposite direction of the AW and eventually exiting Gibraltar (Pinardi and Masetti, 2000). Over the eastern EMed, the circulation of the intermediate depth (Figure 1B) is consistent with the surface (Pinardi et al., 2015). Exiting the Cretan Passage and Kythira Strait, the LIW branches into three streams (Pinardi et al., 2015): the first turns east towards the Levantine, the second southward to the SG, and the third towards the Adriatic. The latter is influenced by the NIG, which strongly enhances (reduces) the flux during cyclonic (anticyclonic) phases (see also Menna et al., 2019), whereas the branch that joins the SG arises as the preferred path of the LIW westward (Pinardi et al., 2015). In the WMed, part of the LIW enters the Western Mediterranean through the Sardinia Channel and directly reaches Gibraltar (Puillat et al., 2006), while the other part flows cyclonically along the Tyrrhenian border and finally exits across the Corsica Channel (Figure 1B). The latter, before reaching Gibraltar, flows cyclonically around the LGG, playing a critical role in dense water formation (Pinardi et al., 2023).

1.3 Sea level in the Mediterranean Sea

According to Pinardi et al. (2014), five terms contribute to the mean sea level change when limited areas of the world ocean are considered, such as the semi-enclosed Mediterranean Sea: (i) the mass fluxes at the open boundaries, accounting for the net volume transport at Gibraltar that alters the mass in the domain; (ii) the net changes linked to the loss or addition of water by surface processes (driven by processes such as evaporation, precipitation, and river runoff within the domain); (iii) the density changes induced by salinity changes (halosteric effect); (iv) the density changes induced by changes in heat flux (thermosteric effect); and (v) the density advection term. The latter, however, is several orders of magnitude smaller than the other four terms, and thus can be considered negligible (Pinardi et al., 2014). The first two terms are defined as incompressible terms that, for simplicity, can be referred to as the mass component. The combined variability of the thermosteric and halosteric effects is referred to as the steric component. The latter fluctuates periodically around zero and is superimposed on the mass component characterized by a yearly and seasonal imbalance between terms (i) and (ii), giving rise to the regional mean sea-level tendency (Pinardi et al., 2014).

The mass component is considered the dominant contributor to the mean sea-level trend in the Mediterranean Sea (Calafat et al., 2010; Pinardi et al., 2014), while the steric component accounts for approximately 20% of the total variance (Calafat et al., 2012). This contrasts with the steric influence at the global scale, which explains approximately 50%–70% of the total sea level variability (Storto et al., 2019). However, there are large differences across the Mediterranean. For instance in the Aegean and Levantine the steric component explains approximately 52% (Mohamed and Skliris, 2022), mainly due to the thermosteric effect (Vera et al., 2009). A direct relationship between sea surface temperature and sea level in the Mediterranean has been demonstrated in previous studies (Cazenave et al., 2001; Cazenave et al., 2002; Fenoglio-Marc, 2002), highlighting a continuous and positive trend associated with sea surface temperature from 1992 to 1999 and for all sub-basins, except for the Ionian.

Large-scale climatic modes also influence long-term and inter-annual variability of the Mediterranean sea level (Vigo et al., 2011; Calafat et al., 2012; Landerer and Volkov, 2013; Tsimplis et al., 2013), such as the North Atlantic Oscillation (NAO) and the Atlantic Multidecadal Oscillation (AMO). For example, NAO positive and negative phases influence precipitation, air temperature, and sea level from local (Meli et al., 2021; Meli and Romagnoli, 2022; Romagnoli et al., 2022) to European scales (Mariotti and Dell'Aquila, 2012; Criado-Aldeanueva and Soto-Navarro, 2020). In particular, the NAO drives atmospheric sea-level pressure changes in the Mediterranean (Tsimplis and Josey, 2001) and alters wind and oceanic circulation near Gibraltar, influencing the net water flux exchange with the Atlantic Ocean (Menemenlis et al., 2007; Tsimplis et al., 2013). Instead, the AMO significantly correlates with heat and salt content (Iona et al., 2018), influencing sea surface temperature and evaporation (Marullo et al., 2011). However, the role of these large climatic modes, despite their importance on the Mediterranean variability at a multidecadal time scale (Calafat et al., 2022), has a limited effect on the quasi-decadal time scale variability (Menna et al., 2022) and is not fully appreciated when short time series are considered (as in the case of satellite altimetry).

Moreover, the sea-level trend can be considerably influenced at regional scale by the contribution of glacial isostatic adjustment

(GIA), the gravitational, rotational, and deformation (GRD) effects, and the dynamic component of sea level, induced by the lateral mass transport. In the Mediterranean Sea the GIA contribution is relatively small (-0.3 mm/yr, Melini and Spada, 2019), while the GRD effects contributed by about 1.5 ± 0.2 mm/yr over the period 2000-2018 (Calafat et al., 2022). For simplicity, all these terms, plus the contribution of large-scale modes and the mass component, from hereon is referred to as the "non-steric effects".

Strong differences in sea-level trends at the sub-basin scale are a well-known aspect of the Mediterranean (Bonaduce et al., 2016; Skliris et al., 2018; Mohamed et al., 2019a), in which variability and complexity arise from thermohaline changes and local circulation (Menna et al., 2012; Mauri et al., 2019; Menna et al., 2019; Menna et al., 2021; Poulain et al., 2021). For instance, the Ionian has in general a negative sea-level trend (Cazenave et al., 2002; Fenoglio-Marc, 2002), in contrast to other sub-basins, primarily because of complexities and changes in the local circulation pattern (Malanotte-Rizzoli et al., 1997; Pinardi et al., 1997; Malanotte-Rizzoli et al., 1999).

Regarding non-linearity in sea-level trends, an abrupt change was observed around 1999, leading to a loss of correlation between sea surface temperature and sea level after that year (Vigo et al., 2005). Furthermore, the Ionian began to be characterized by a rising trend after 1998, which was attributed to the switch of surface circulation from anticyclonic to cyclonic (Gačić et al., 2010) after the relaxation of the EMT (Vera et al., 2009, see also Section 1.1). After that period and since the early 2000s, a non-linear behavior has been observed in sea-level trends, where a rising condition peaked in 2003, followed by a drop until 2009 (Vigo et al., 2011).

2 Materials and methods

2.1 Data

Gridded daily mean sea-level anomalies (SLA) at 1/8°x1/8° spatial resolution over the Mediterranean Sea for 1993–2019 were obtained from the Copernicus Climate Change Service (C3S). The dataset was delivered by the DUACS altimeter production system, which includes data from several altimetry missions, but always merging a steady number (two) of altimetry measurements at the same time. This procedure avoids introducing biases and provides stability and homogeneity of the record over the entire period, which is crucial for climate applications and long-term evolutionary analyses (Legeais et al., 2021). All standard corrections (e.g., signal refraction passing through the atmosphere, sea state bias, instrumental drift, and dynamic atmospheric correction) were applied to the dataset (for details, see Taburet et al., 2019).

Monthly average temperature and salinity vertical profiles were obtained from the Mediterranean Sea Physics Reanalysis dataset (Escudier et al., 2020), distributed by the Copernicus Marine Environment Monitoring Service (CMEMS; available at the url: https://marine.copernicus.eu/). This dataset covers the period 1987–2020, and it has a spatial grid resolution of 1/24°x1/24° and 141 vertical levels (unevenly spaced). The physical dynamics of the Mediterranean Sea are modeled using an Ocean General Circulation Model (OGCM) that is based on the Nucleus for European Modelling of the Ocean (NEMO) code (Madec et al., 2017). This numerical model is used to solve the primitive equations of motion that describe the movement of water in the Mediterranean Sea. The water balance is computed using the difference between evaporation, derived from latent heat flux data, and the combination of precipitation and rivers runoff, derived from various datasets (Escudier et al., 2021 and references therein). The connection with the Marmara Sea is modeled as a river (Kourafalou and Barbopoulos, 2003), while the exchanges at Gibraltar are resolved by extending the model into the north-east Atlantic Ocean. Temperature and salinity observations are assimilated into the system through the OceanVar data assimilation scheme (Dobricic and Pinardi, 2008), which includes *in-situ* vertical profiles from the Argo profiling floats, CTDs, and XBTs from SeaDataNet (https://www.seadatanet.org/) and CMEMS (INSITU_GLO_NRT_OBSERVATIONS_013_030) database. Details of this reanalysis dataset are discussed in Escudier et al. (2021).

2.2 Methods

To cope with the large oceanographic and bathymetric variability characterizing the Mediterranean Sea, the time series analysis at the sub-basin scale was made by following the same partitioning (Figure 1A) outlined by Carillo et al. (2012) and Galassi and Spada (2014). The C3S altimetry observations were corrected for GIA using the geoid height estimates (dGeoid) from the ICE-6G_C (VM5a) model (Argus et al., 2014; Peltier et al., 2015), was applied to the C3S altimetry observations as a correction for the GIA effect. Furthermore, to account for the altimeter instrumental drift that influences the accuracy and uncertainty of the records between 1993 and 1998 (Watson et al., 2015; Beckley et al., 2017; Dieng et al., 2017), a TOPEX-A instrumental drift correction (WCRP Global Sea Level Budget Group, 2018), derived from altimetry and tide gauge global comparisons, was added to the C3S sea-level datasets. Although this correction is computed for the global mean sea level, it can also be used at a regional or local scale as the best available estimate. This is still preferable to not correcting at all, given that the regional variation of the instrumental drift is currently unknown.

The Thermodynamic Equation of Seawater (TEOS-10, McDougall and Barker, 2011) was used as the equation of state to compute the steric sea-level component, following Camargo et al. (2020). The steric (η_s) computation is based on the vertical integration of density anomalies from the maximum local depth (-H) to the water surface (0), following Gill and Niller (1973) and Tomczak and Godfrey (2003):

$$\eta_s = -\frac{1}{\rho_0}\int_{-H}^{0}\rho' dz$$

where ρ' and ρ_0 are the local and reference density anomalies, respectively. The former is a function of temperature and salinity variations retrieved from the reanalysis dataset (see Section 2.1).

Before computing steric anomalies, potential temperature and practical salinity values are converted to conservative temperature and absolute salinity (McDougall and Barker, 2011; McDougall et al., 2012). In addition, the thermosteric and halosteric effects were also computed and analyzed individually to better appreciate the influence and evolution of both effects.

Due to the different temporal coverage of the datasets, we restricted the analyses to the common period from January 1993 to December 2019. Daily time series were converted into monthly and annual means. Moreover, the mean seasonal cycle was removed from all the monthly mean time series. To ensure a full comparability between the datasets, the steric, thermosteric, and halosteric datasets were regridded from 1/24° to 1/8°, i.e. the resolution of the altimetry data, using the First-Order Conservative Remapping method (Jones, 1999), which is implemented in the Climate Data Operators software.

A non-parametric Mann–Kendall test (Mann, 1945; Kendall, 1975), modified for autocorrelated data (Hamed and Rao, 1998), was performed to assess the statistical significance of trends at the 95% confidence interval. The Mann-Kendall test was implemented with the non-parametric Theil–Sen estimator (Theil, 1950; Sen, 1968) to evaluate the preferred slope from the simple linear regression computed for each time series. The resulting preferred slope was assumed to be a constant trend (or rate) of the time series over the selected period. Associated error is determined from the distribution of values. In principle this can be not normal and lead to a not symmetric associated error bar. To ease the reading and result interpretation, we assign a conservative symmetric error by choosing the largest one.

In this analysis, the Binary Segmentation algorithm (Scott and Knott, 1974; Sen and Srivastava, 1975) was used to search for the unknown epoch of change points in the altimetry monthly time series (de-seasoned, TOPEX-A and GIA corrected). This is among the most-competitive methods for change point analysis (Cho and Fryzlewicz, 2015; Rice and Zhang, 2022). The algorithm uses a cost function, namely the Radial Basis function (Harchaoui and Cappé, 2007), to search for the preferred epoch at which the change point should be set. Then it uses the change point to split the time series in two sub-series and it iterates the change point search process until a predefined stopping criterion (here defined as the max change point number equal to three) is reached (Truong et al., 2020). Figure 2A show the detection of change points on a single time series. The Radial Basis Function was preferred since it belongs to the kernel-based methods and it is suitable for performing change point detection in a non-parametric setting (Harchaoui and Cappé, 2007); this model is particularly useful when the change points are suspected to be irregularly distributed in the time series (Killick et al., 2012; Truong et al., 2020). Offsets were not present in the considered dataset.

The detected change points (three for each time series) were then aggregated at the basin scale, to create a cumulative distribution (Figure 2B). The occurrence of a change point cannot be precisely attributed to a single moment in time, as it may be influenced by a variety of processes that induce a spatially and temporally varying response in sea level. As a consequence, only distributions exceeding the 75th percentile were considered and selected (represented by black bars in Figure 2B), accompanied by their respective reference medians (indicated by hatched vertical red lines in Figure 2A). Each median, accompanied by an arbitrary error margin of ± 1 year (depicted as a red shaded area in Figure 2B), provided an effective means of clustering the major distributions into four distinct groups, which were centered around the years

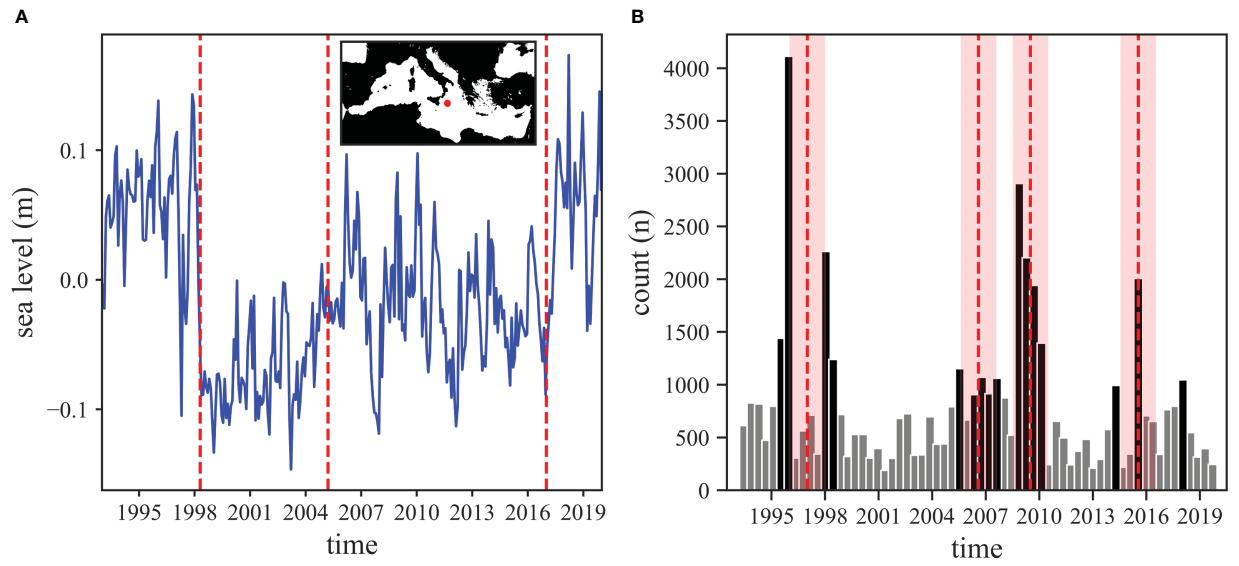

FIGURE 2
Left panel **(A)** shows one sample of monthly mean sea level time series from the Ionian region (marked by the red dot in the inset map. Red hatched lines mark the three most likely change point detected by the algorithm described in Section 2.2. The right panel **(B)** displays the cumulative distribution (grey bars) for the whole set change points detected in altimetry monthly time series throughout the Mediterranean Sea. Black bars mark the subset of distributions exceeding the 75th percentile. For each selected distribution, the median (hatched red lines) defines the selected change point while an arbitrary error of ± 1 year (shaded in red) was introduced to account for potential uncertainties in the analysis.

1997, 2006, 2010, and 2016. The two distributions localized around 2014 and 2018 were excluded from this clustering, as their proximity to the 2016 cluster makes them unusable for the analysis.

To properly account for autocorrelation and clean the signal from interannual variability, the time series were converted into annual means and the modified Theil-Sen estimator was used to calculate trends and errors for each sub-series. Subsequently, the statistical significance (at the 95% confidence interval) of each change point was evaluated for each time series by applying a Fisher F-test to the Chow statistics (Chow, 1960; Winer, 1962; Olivieri and Spada, 2013).

3 Results and discussion

3.1 Linear trend analysis

Figure 3A shows a large spatial variability of the rate of sea-level rise derived from satellite altimetry (total sea level) for the period 1993–2019, confirming observations by Bonaduce et al. (2016), despite the different time windows. The highest positive rates (from ca. 3 to 4 mm/yr and above) are observed over the Aegean and Levantine, especially in regions where recurring gyres and eddies in the circulation are present (PG, MMGS, and SGS in Figure 1B). Conversely, negative rates (down to over -4 mm/yr) are observed in some portions of the Ionian, corresponding to the NIG and along the MIJ, and largely in the Southern Crete along the MMJ and IG; the latter represents the area with the largest negative rate observed throughout the Mediterranean Sea. At the Mediterranean basin scale, the average sea-level trend is 2.1 ± 0.5 mm/yr (95% confidence interval), comparable with Mohamed et al. (2019a). However, long-term linear trends of total sea-level change at the sub-basin scale (see also Section3.2) confirm the variability observed in Figure 3A as the consequence of local processes. In detail, values of 1.8 ± 0.6, 2.1 ± 0.8, and 2.5 ± 0.6 mm/yr are observed for the Western Mediterranean, Southern Central Mediterranean, and Tyrrhenian, respectively. Higher trends (albeit comparable within the ranges) are observed for the Adriatic (2.6 ± 0.8 mm/yr), Levantine (2.6 ± 0.9 mm/yr), and Aegean (3.1 ± 1.0 mm/yr), consistent with Mohamed and Skliris (2022), who found an average rate of 3.23 ± 0.61 mm/yr for the eastern EMed over the same period. Conversely, trends for the Ionian (1.6 ± 1.6 mm/yr) and Southern Crete (0.3 ± 1.3 mm/yr) are non-significant.

The significance of the rate obtained from the trend analysis is considered by plotting the spatial distribution of the statistics at the 95% confidence interval (CI) in Figure 3A. Dots represent regions where the null hypothesis cannot be rejected, that is, the significance of the resulting rate cannot be statistically confirmed. This can be associated with a null rate and significant changes in the time series that diverge from the linear model. Notably, these time series have no significant trend clusters in specific sectors of the Mediterranean Sea, suggesting that it cannot be the consequence of a random process but, conversely, related to local dynamics, such as the influence of gyres/eddies or currents. In detail, a lack of significance in the Western Mediterranean is observed for sea-level trend from altimetry in the EAG-Balearic Islands area (hereafter refer to Figure 1 for location). A very large portion of the Ionian also denotes weak or non-significant rates, especially in conformity with the NIG, AIS, and along MIJ. When moving toward the east, a lack of significance is observed in correspondence with the PG, in a large part of Southern Crete, and a spot within the SGS. However, the significance in the IG is noteworthy, representing the only statistically significant negative rate in the entire Mediterranean Sea from 1993 to 2019.

Steric sea-level trends (Figure 3B) also show wide spatial variability, described by a progressive increase from west to east.

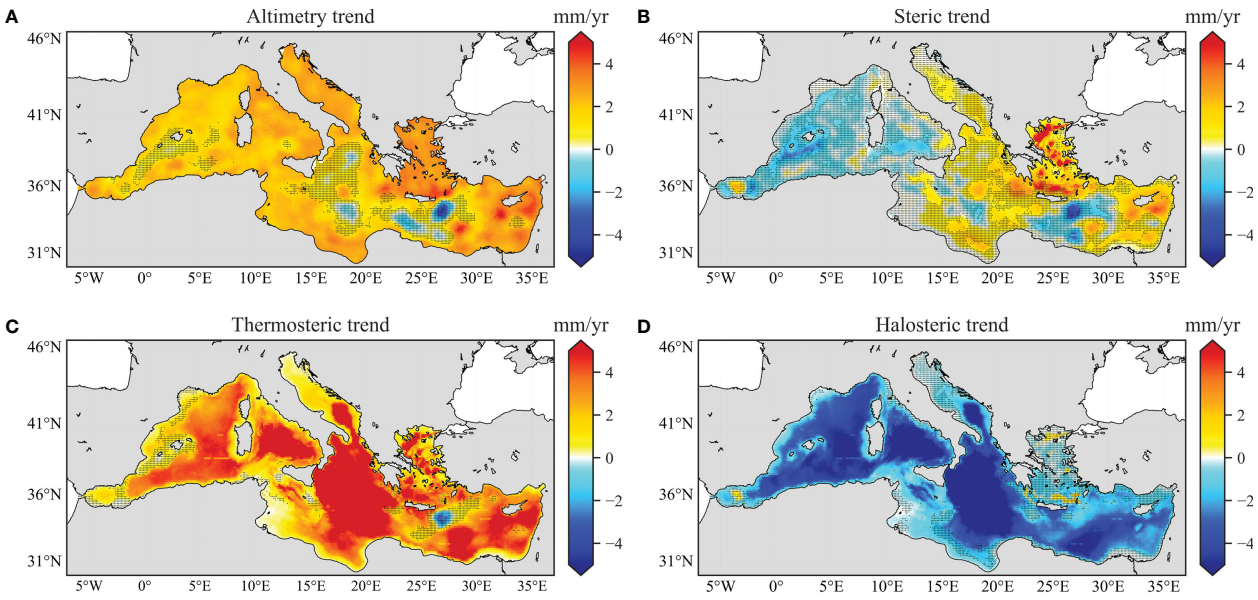

FIGURE 3
Trends of total sea level **(A)**, steric **(B)**, thermosteric **(C)**, and halosteric **(D)** components, computed over the satellite altimetry era (1993–2019). Black dots mark areas in which the trend is non-significant (95% CI).

General negative trends are observed throughout the WMed, except for WAG. A behavior similar to altimetric trends is observed in the Ionian, where low values are aligned along the AIS and MIJ. Weak positive values characterized the Adriatic, whereas the Aegean shows higher positive trends linked to the steric component of the entire Mediterranean Sea. As for altimetry, steric trends in the Levantine and Southern Crete can be split into positive and negative trends, respectively, and negative trends are shown along the MMJ, with the most prominent (down to -4.5 mm/yr) at the IG.

The statistical significance of the steric component trends (Figure 3B) tends to be absent throughout the Mediterranean Sea, characterized by an average non-significant rate of 0.3 ± 0.6 mm/yr. While almost all sub-basins show a non-significant steric sea-level trend, the presence of significant trends denotes a patchy pattern. A few exceptions are the Aegean (2.1 ± 1.3 mm/yr), Levantine (1.1 ± 1.0 mm/yr), and Southern Central Mediterranean (1.0 ± 0.8 mm/yr), in which the average spatial trends are significant, albeit spatially uneven. These values denote an influence of the steric component on the total sea-level change of approximately 68, 42, and 48%, respectively, for the three sub-basins, consistent with Mohamed and Skliris (2022), who reported that 52% of the total sea-level change in the eastern EMed was due to steric effects. In this case, the behavior of the three sub-basins is consistent with the global mean, where the steric component accounts for approximately 44% of the total sea-level change over the period 1993-2017 (Storto et al., 2019). In contrast, the steric component in the other sub-basins contributes negatively to the long-term total sea-level trend, except for the Adriatic and Ionian, where it accounted for approximately 15 and 31%, respectively. This highlights how a large part of the long-term sea-level trend within the Mediterranean Sea, except for the eastern EMed, is driven by non-steric effects (ca. 86%). This is consistent with previous studies, who found an influence of the steric component over the Mediterranean of less than 20% and that the mass component becomes the dominant element for regional sea-level trends (Calafat et al., 2010; Calafat et al., 2012; Pinardi et al., 2014).

Thermosteric trends (Figure 3C) are generally positive throughout the domain, with high values (>3–4 mm/yr) observed in the Ionian (5.3 ± 1.0 mm/yr), Tyrrhenian (3.0 ± 0.6 mm/yr), Levantine (3.3 ± 1.1 mm/yr), Southern Central Mediterranean (3.4 ± 0.6 mm/yr), and Aegean (2.8 ± 1.0 mm/yr). The IG is the only region with negative thermosteric values, which contributes to lowering the average rate of the Southern Crete (2.4 ± 1.1 mm/yr). Most of the thermosteric rates over the Mediterranean Sea are statistically significant (average rate of 2.8 ± 0.5 mm/yr), including the IG negative rate, and except for the PG, MMJ-RG alignment, and the EAG-Balearic Islands region. Lower but significant thermosteric trends are observed over the Adriatic (1.9 ± 0.6 mm/yr) and Western Mediterranean (2.0 ± 0.6 mm/yr).

In contrast, the halosteric effect (Figure 3D) is characterized by negative trends (increasing water column salinity, leading to an increase in sea water density and related volume reduction) in all sub-basins, with some small spots showing a weakly positive trend in the Aegean and WAG. At the sub-basin scale, the Aegean shows a not statistically significant trend of -0.6 ± 0.9 mm/yr, whereas the Adriatic (-1.5 ± 0.5 mm/yr), Southern Central Mediterranean (-2.4 ± 0.5 mm/yr), Tyrrhenian (-2.5 ± 0.7 mm/yr), and Levantine (-2.0 ± 0.8 mm/yr) have a significant negative trend. Generally, halosteric trends contribute negatively to the total altimetric sea level across almost the entire Mediterranean Sea (-2.5 ± 0.3 mm/yr). Stronger negative trend is observed for the Ionian (-4.9 ± 1.3 mm/yr).

Thermosteric trends are often higher than the total sea level trends; however, their overall contribution to the steric component is strongly influenced and lowered by the negative contribution of the halosteric effect. The opposite contributions of these two effects have been observed throughout the eastern EMed (Mohamed and Skliris, 2022) and the North Atlantic Ocean (Storto et al., 2019). This opposite effect is the direct outcome of the progressive regional increase in water temperature and salinity (Romanou et al., 2010; Pastor et al., 2018; Skliris et al., 2018; Grodsky et al., 2019; Mohamed et al., 2019a; Pisano et al., 2020; Menna et al., 2022). Additionally, this opposite behavior is the cause of the generalized non-significance of the steric component over the entire Mediterranean Sea, as the two opposite effects almost cancel each other out (Passaro and Seitz, 2010). This highlights the extent to which the halosteric effect is influential within semi-enclosed basins at mid-latitudes, conversely to the global ocean where the thermosteric effect represents the dominant driver of steric component variability (Robinson et al., 2001; IPCC, 2021).

3.2 Mediterranean sea-level inflections

Following the four change point clusters detected (1997, 2006, 2010, and 2016), each of the variables are reanalyzed for the sub-periods (1993-1997, 1997-2006, 2006-2010, 2010-2016, 2016-2019). Figure 4 shows the spatial difference that characterizes each point of the grid for each variable considered (i.e., total sea level from altimetry, steric component, thermosteric, and halosteric effects) between two different sub-periods separated by a selected change point that acts as a pivotal point in the time series. A positive (negative) value suggests an acceleration (deceleration) in sea-level change at a specific location. This could also reflect a sign variation, namely from negative to positive or vice versa, or just an increase or decrease in the observed rate. For each of the four change points, both the complete map of the trend changes (to have an overview and intensity of the process) and the map with only the statistically significant trend changes at 95% CI, as determined through the Chow test (see Section 2.2), are shown. The latter means that any points which change of trend is considered statistically valid, and thus better represented by a bilinear model rather than by the simple linear model. From hereon, for simplicity, the term "inflection" is defined as a change in rate, positive or negative, occurring in a time series in a specific pivotal year.

On the other hand, Figure 5 shows the temporal evolution, with related significant inflections, of the variables considered at the sub-basins scale. The time series of average annual mean sea level from altimetry for the entire Mediterranean Sea (Figure 5A, solid black line) highlights how the sea level is rising, unlike the steric component (dashed yellow line), which shows a weak and an overall non-significant positive trend, consistent with the map in

10.3389/fmars.2023.1150488

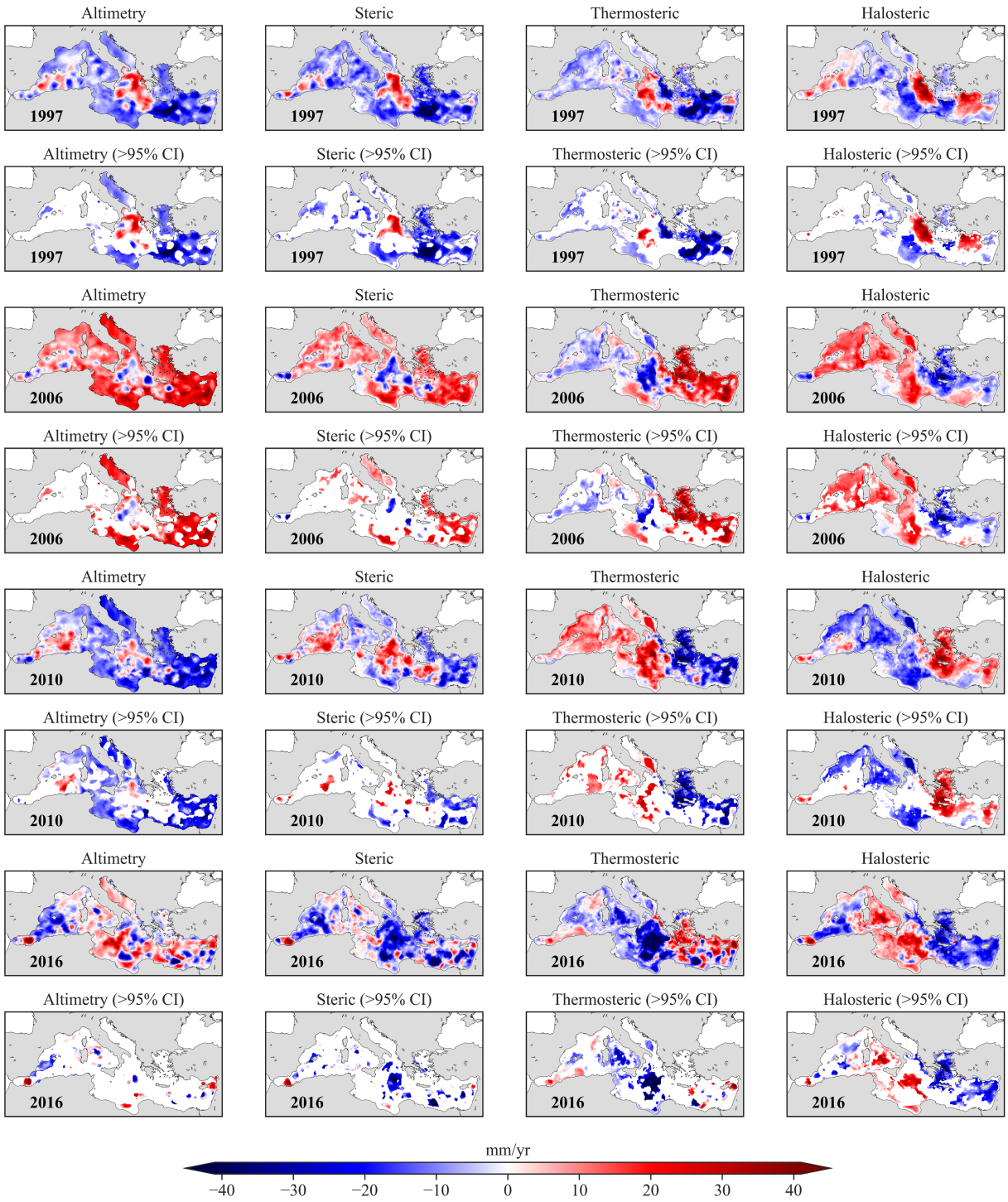

FIGURE 4
Rate variations from yearly mean time series for each of the four years (1997, 2006, 2010, and 2016) resulting from the change point analysis for (from left to right column) the total observed sea level from altimetry, steric component, and thermosteric and halosteric effects. Each inflection of trends is shown both overall, at the scale of the Mediterranean basin, and only in those sectors where the statistically significant (>95% CI) change of trend occurred. Positive (negative) inflections are shown in reddish (bluish) colors, corresponding to increased (decreased) sea-level trends at a specific location after the given year (statement in bold in the lower left corner of the maps).

Figure 3B. Opposite trends of thermosteric and halosteric components (red dotted and blue dash-dotted lines, respectively) over the Mediterranean Sea denote considerable rising and decreasing trends, respectively (see also Figures 3C, D).

3.2.1 The 1997 inflection

The spatial distribution of the 1997 inflection shows a marked bimodal behavior at the basin scale (Figure 4) with positive inflection over a large portion of the Ionian and negative values

10.3389/fmars.2023.1150488

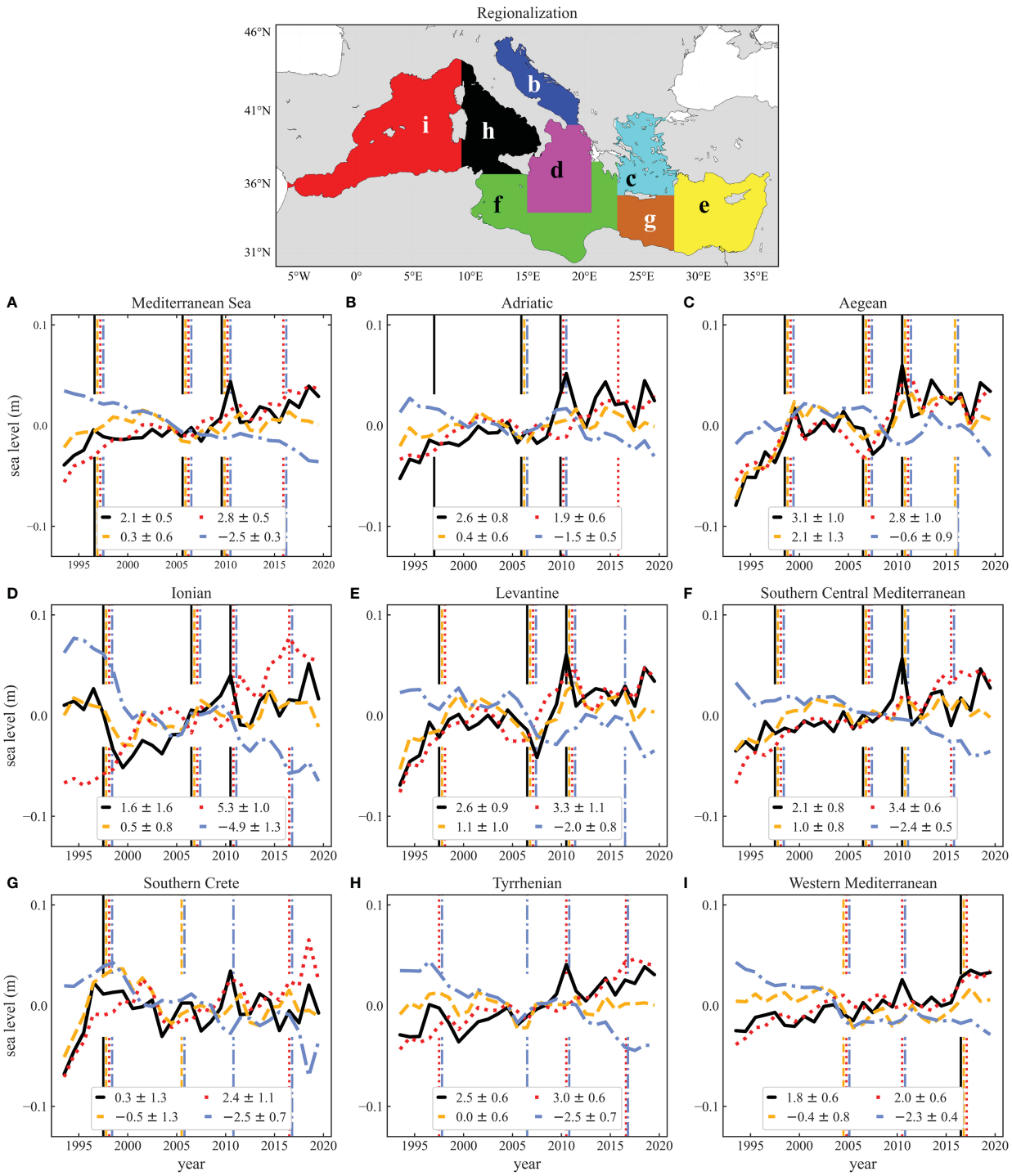

FIGURE 5
Annual sea level time series from altimetry (black solid line), steric (dashed yellow), thermosteric (dotted red), and halosteric (dash-dotted blue) components over different spatial scales (see also map at the top of figure): Mediterranean Sea **(A)**, Adriatic Sea **(B)**, Aegean Sea **(C)**, Ionian Sea **(D)**, Levantine Basin **(E)**, Southern Central Mediterranean **(F)**, Southern Crete **(G)**, Tyrrhenian Sea **(H)** and Western Mediterranean Basin **(I)**. Vertical lines denote significant changepoint in the related component (same color and line style) at a specific time. Trends refer to the period 1993–2019.

that characterize most of the EMed. The WMed is characterized by non-uniform behavior. Considering the entire Mediterranean basin, an average negative inflection of ca. -6.9 mm/yr occurs between 1993–1997 and 1997–2006. Most of the positive inflections over the Ionian (Figure 5D) and negative ones in the Aegean (Figure 5C), Southern Crete (Figure 5G), Levantine (Figure 5E), and Adriatic (Figure 5B) are statistically significant (see also Figure 4). Furthermore, part of the Southern Central Mediterranean also has significant negative inflections. Changes in the steric trends in 1997 show a large similarity to altimetry regarding spatial

distribution and statistical significance; indeed, the steric negative inflection at the scale of the Mediterranean Sea is -6.7 mm/yr, in agreement with the altimetric value.

Both thermosteric and halosteric effects show a positive inflection in a large part of the Ionian, albeit not overlapping but characterizing opposing sectors, that is, south-west for the thermosteric and northeast for the halosteric, with the latter almost entirely significant. In contrast, inflection owing to the thermosteric element, apart from the Ionian, shows negative values for the entire Mediterranean Sea, with large areas of significant inflection in the Levantine. Similarly, the halosteric inflection denotes areas with a significant change in trend: positive values, besides the eastern Ionian, characterize large parts of the Levantine and Western Mediterranean regions, while the negative ones are particularly relevant in the Southern Central Mediterranean. The thermosteric effect inflection at the Mediterranean scale accounts for approximately 97% of the steric component inflection, whereas the remaining 3% is attributable to the halosteric effect.

The time series representative of the Ionian (Figure 5D) denotes a unique non-linear behavior in the altimetry, with an abrupt and significant positive inflection around 1997 for all variables. The 1997 positive inflection that characterizes the Ionian, for total and steric components, represents a direct consequence of the switch of NIG from anticyclonic to cyclonic circulation after EMT relaxation (Vera et al., 2009; Gačić et al., 2010). The total sea level in the Ionian is therefore characterized by a long-term rising trend when only data from 1997 are considered (see also Vera et al., 2009), and the strong inflection that occurred in 1997 is the cause of the lack of significance in the Ionian trend over the period 1993-2019 (observed in Figure 3A).

According to Vigo et al. (2005), the changes of state in the thermohaline circulation in this phase led to a 'breathing' oscillation, possibly linked to an in-phase cooling/heating of the whole Mediterranean Sea or a loss/addiction process of water mass; this is also observed in this study for total and steric 1997 inflections across the whole EMed (Figure 4), where all sub-basins trends move up and down in phase, reaching a peak-to-peak amplitude of approximately 10 cm. Conversely, no significant inflections arise in the WMed (Figures 4, 5H, I), confirming the observations of Vigo et al. (2005).

The shift to a cyclonic phase led to the reinforcement of the AW flux along the MIJ towards the Levantine, thus diluting the surface waters and modifying the thermohaline properties of the latter (Gačić et al., 2011; Gačić et al., 2014), possibly becoming fresher and cooler. During the cyclonic phase, the AW reaches Levantine, traveling eastward directly from the Sicily Channel. The related consequences can be observed in Figure 4, where significant 1997 inflections in Levantine are negative for the thermosteric effect (water contraction due to lower temperature) and positive for the halosteric effect (water expansion due to lower salinity), especially in the RG. The latter represents the area of the main formation of the LIW (Pinardi et al., 2015 and references therein) which then flows westward through the Cretan Passage and Cretan Sea (entering and exiting the Kasos and Kithira straits, respectively), which explains the generalized, significant positive (negative) inflection that characterizes the eastern Ionian (Figure 4), where fresher (cooler) waters were carried toward the northwest along the LIW path. Conversely, the thermosteric effect provides a significant positive inflection along the western flank of the Ionian, ascribed to the replacement of the AW masses (deflected toward the northern Ionian during the previous anticyclonic phase) with those from the Levantine, with a long period to heat up and are relatively warmer than the AW that directly enters the Sicily Channel. This also influenced the Adriatic water properties, especially at the SAG, where relatively saltier waters from the Levantine replaced the AW, which had previously arrived directly from the Sicily Channel during the anticyclonic phase (see also Gačić et al., 2013). For the Adriatic, however, a significant negative inflection is observed in the altimetry, which cannot be explained by the steric component (Figures 4, 5B). It can be argued that the altimetry inflection was caused by the reduction of the AW mass amount entering the Otranto Strait after the cyclonic regime was established. However, the influence of internal processes (e.g., river discharge) within the sub-basin during this phase cannot be excluded.

Finally, the effect observed in the Southern Central Mediterranean was mainly linked to the salinization of the area around the SG, leading to a significant negative inflection, ascribed to the southward path of the LIW (Figure 1B), that is, the preferred path towards the Sicily Channel (Pinardi et al., 2015), which joins the SG and flows along the Gulf of Sirte shelf break and eventually exits the EMed (Sparnocchia et al., 1999; Pinardi et al., 2006). As the salinity of the SG area during cyclonic phases generally increases, it suggests that the intermediate depth waters flowing towards the Sicily Channel (see also Schroeder et al., 2017) drive the steric sea-level change over this area, despite the presence of AW that flows along the SSTC at the surface.

3.2.2 The 2006 inflection

Considering the change point occurrence in 2006, the inflections on the altimetric rate are again distributed according to a well-defined pattern, consistent with the steric component. In detail, a relatively bimodal behavior is shown, similar to the 1997 inflection but showing the opposite phase condition, with the Ionian characterized by negative values, in contrast to all the other regions that showed positive values (Figure 4). In addition, statistical significance is found for altimetry, corresponding with the NIG for negative values and large portions of the EMed for positive values. Overall, this inflection at the Mediterranean scale led to a generalized positive change of sea-level trend of approximately 11 mm/yr, with about 50% explained by the steric trend inflection, which reached 5.5 mm/yr.

The thermosteric and halosteric inflections show a generalized behavior of opposite signs. The distribution of significance for the two effects shows different patterns, with the thermosteric significance limited to some specific areas, while the halosteric one covers a large portion of the Mediterranean Sea. Furthermore, the halosteric effect at this stage explains approximately 31% of the steric component variability; hence, it has a greater influence than the case of the 1997 inflection. Specifically, for the 2006 inflection, a marked and homogeneous opposite behavior of thermosteric and halosteric effects is shown in the WMed.

The inflection detected in 2006 might be the response of sea level to the switch of the NIG to an anticyclonic from a cyclonic state. Cyclonic circulation, established around 1997, shifted again to anticyclonic circulation in 2006 (Gačić et al., 2014). The onset of an opposite behavior in NIG circulation led to a further breathing oscillation throughout the EMed, with all sub-basins moving up and down in the reversed phase for 1997. The peak-to-peak amplitude for this inflection point decreased about 1 cm in comparison to the previous inflection, reaching values of approximately 9 cm for both the altimetry and steric components.

The shift to anticyclonic NIG circulation also led to opposite inflections of thermosteric and halosteric sea-level trends (Figure 4) for 2006. During this phase, the western Ionian interior was replenished by the colder and fresher AW that mainly advected northward (Robinson et al., 1999), entering the Adriatic, affecting the sea surface temperature and salinity. The halosteric provides a significant (positive) inflection throughout the whole sub-basin, decreasing the water density in the whole Adriatic, thus driving a positive steric inflection. However, it is not strong enough to fully explain the marked, significant positive inflection observed in the altimetry over the Adriatic, suggesting that an opposite mechanism, with respect to 1997, impacted the sub-basin.

A possible mechanism could be a greater replenishment of AW masses, which directly entered the Otranto Strait in the anticyclonic context. The direct AW flow towards the Cretan Passage was greatly reduced owing to the absence (or drastic weakening) of the MIJ caused by the anticyclonic Ionian meander (Gačić et al., 2011). This state led to a generalized freshening of the Southern Central Mediterranean (driving the halosteric trend change), as the portion of AW not deflected northward branched into the SSTC and SG (Lermusiaux and Robinson, 2001; Onken et al., 2003). Thus, we can hypothesize that, during this phase, surface circulation is the dominant driver of steric changes. Furthermore, this state also led to salinization and warming of the Levantine because of the longer pathway of the AW reaching the eastern EMed (Manca, 2000).

As observed for the 1997 inflection, significant changes occurred around RG, influencing (this time with a negative halosteric inflection) the formation of the LIW. A lower dilution context increased the LIW salinity, leading to Aegean salinification with the LIW passing through the Cretan Sea and eastern Ionian (Theocharis et al., 1999). However, the significant positive inflection of the thermosteric effect in the Aegean and Levantine regions, caused by the sea surface temperature increase during this phase, seems to be the main driver of the inflection observed in the steric component.

The observations on the WMed time series (Figures 5H, I) and the spatial distribution of significant inflections (Figure 4) show negative and positive inflections for thermosteric and halosteric effects, respectively. The 2006 inflection is not reflected in the altimetric signal over the WMed and, in the Western Mediterranean, seems to start earlier, around 2004. This could be linked to the Western Mediterranean Transition (WMT, Roether et al., 1996), that was linked to a thermohaline anomaly that occurred around 2004–2005 and spread throughout the WMed, inducing freshening and cooling in the deep and intermediate layers (Schroeder et al., 2010; Zunino et al., 2012; Schroeder et al., 2016). This agrees with our observations in Figure 4, especially with the generalized positive, significant inflection in the halosteric effect.

3.2.3 The 2010 inflection

For the 2010 inflection, a well-defined bimodal behavior of the sea-level trend is also observed, and a good agreement between the altimetry and steric component regarding spatial variability (Figure 4). The main pattern is very similar (but with a more patchy distribution) to that observed for the 1997 inflection when the same type of reversal (i.e., from anticyclonic to cyclonic) in the NIG circulation occurred (Gačić et al., 2014). In detail, positive values characterize the Ionian, whereas generalized negative values are representative of the entire remaining EMed. Conversely, in WMed, the pattern appears randomly distributed but with a more substantial positive value. Most of the Mediterranean shows significant inflections in altimetry, especially in areas with negative values, almost the entire Adriatic, Levantine, and Southern Central Mediterranean. Positive significance emerges only corresponding to the NIG, PG, and over part of the Western Mediterranean region. The 2010 inflection, at the scale of the Mediterranean Sea, provides an average negative value of approximately -8.9 mm/yr, which is lower but similar to the 1997 inflection. In this case, the steric inflection is weaker than the variation observed in the total sea level, reaching about -1.6 mm/yr. The peak-to-peak amplitude remains the same as in 2006 for the altimetry and steric components, with a value of approximately 9 cm. Conversely, the contribution of the non-steric effects to the 2010 inflection seems to increase again (ca. -7.3 mm/yr) but negatively, enhancing the effect of the steric component on the total sea level. Regarding the steric component influence, the thermosteric effect accounts for approximately 68% of the average 2010 steric inflection, similar to that observed in 2006.

A similar behavior to the 1997 of thermosteric and halosteric effects is shown in 2010 in the EMed, while major differences arose in the Adriatic and Aegean, showing some significant inflections with opposite signs than 1997. In detail, the same sea water freshening in the RG area occurred, influencing the LIW properties, which propagated westward through the Cretan Passage and Cretan Sea and eventually changed the salinity of the eastern Ionian and Aegean. The latter, different from 1997, seems to have been impacted entirely by the freshening, while cooling, similar to 1997, is observed. In the Adriatic, the inflections of both effects are noticeable and more marked in 2010 than in 1997, with significant warming and salinization owing to the replacement of the AW (directly entering during the previous anticyclonic phase) with the waters coming from the Levantine. More prominent than in 1997, the generalized negative inflection observed in the altimetry over the Adriatic cannot be ascribed to the steric component, reinforcing the hypothesis advanced in Section 3.2.1 regarding the decrease in the intake of AW masses during the cyclonic phases. Thus, in 2010, as well as for 1997 and 2006 (Figures 4, 5B), for the Adriatic, the significant inflections may have been mainly driven by the non-steric effects as a consequence of the differential contribution of AW masses during NIG shifts.

3.2.4 The 2016 inflection

The 2016 inflection, in contrast to the others previously analyzed, does not provide the same defined pattern throughout the Mediterranean Sea (Figure 4). Instead, it provides a patchy

pattern linked to local gyres and complexities at the sub-basin scale and information about a significant positive inflection in the westernmost portion of the WMed. Despite this detected inflection being close to the subsequent NIG reversal (from cyclonic to anticyclonic), which occurred around 2017 (von Schuckmann et al., 2019), another significant shift (also in this case from cyclonic to anticyclonic) occurred in 2012, probably linked to the extremely cold winter that affected the Adriatic during the same year (Bensi et al., 2013; Mihanović et al., 2013; Gačić et al., 2014), but quickly restored to cyclonic conditions in 2013. This brief reversal episode may have influenced the sea level and the formation of the breathing oscillation, as observed previously. However, further analyses with different time-resolution datasets are required to prove this hypothesis. Furthermore, it should be considered that, in this case, the upper limit of the split series is the end of the time series themselves; therefore, to properly evaluate the effect of the 2016 change point (likely related to the last NIG reversal), it would require considering the entire time interval until the next shift.

At the Mediterranean Sea scale, the 2016 inflection provides an average value of 0 mm/yr, which contrasts with the steric component that is ca. -5.6 mm/yr, of which about 52% is explained by the halosteric effect. This suggests that the impact of the halosteric effect has been further amplified, and that the non-steric elements have positively contributed by approximately 5.6 mm/yr to balance the total sea level budget, as observed in the 2006 inflection. Moreover, similarities with the 2006 inflection can also be observed in the thermosteric and halosteric effects, especially in the EMed (Figure 4).

The significant inflection observed in the Western Mediterranean in 2016 for altimetry (Figure 4) represents the only change point observed in the total sea level throughout the WMed over the period under analysis (Figure 5I), possibly driven by the steric component and, in detail, by the thermosteric effect. This phenomenon can also be linked to the WMT footprint, as suggested by Schroeder et al. (2016) and Naranjo et al. (2017), with a strong acceleration in temperature and salinity trends after 2013 (consistent with the observation in Figure 5I), driven by the Western Mediterranean deep-water formation and flowing out of the Gibraltar Strait.

4 Summary and conclusions

When considering linear modeling, the distribution of sea-level trends across the entire Mediterranean basin (Figure 3A) shows a large spatial variability since 1993, consistent with previous studies (Bonaduce et al., 2016; Mohamed et al., 2019a). Zones of non-significance in the total sea level trend from altimetry (Figure 3A) reflect areas of critical passages of different water masses with related complex circulation at surface and intermediate depths, as in the case of the EAG-Balearic Islands sector, Southern Central Mediterranean, and Southern Crete. Also, the Ionian lacked a significant trend over the whole period; however, it becomes significant when analyzed only since 1997 (as previously observed by Vera et al., 2009), thus the lack of significance in the long-term trend is caused by the abrupt change point within the time series (Figure 5D). Conversely, the lack of significance in the Southern Crete (Figures 3A, 5G) is not due to inflections of opposite signs, which may affect the long-term trend, but this sub-basin is linked to a substantial absence of a trend. This also probably reflects regionalization, as Southern Crete comprehends the Cretan Passage and the IG, which strongly influences sea level. However, a large positive trend before 1997 characterizes all the time series within the sub-basin, denoting a different behavior for 1997–2019. This could be linked to the final phase of the EMT and the restoration of thermohaline cell circulation of the EMed in 1999 (Manca et al., 2003), with the consequent restitution of the pre-EMT situation (Vigo et al., 2005). As for the Southern Crete, the absence of trend in the western WMed is probably linked to the complexity of the area, with incoming AW and outflowing LIW waters heavily impacting sea level.

The steric component, contrary to the global mean sea-level change (Storto et al., 2019), generally slightly affect the total long-term sea-level trend (Figure 3B) in the Mediterranean Sea, which is dominated by the contribution of the non-steric effects explaining approximately 80% of the total variance, consistent with previous studies (Calafat et al., 2010; Calafat et al., 2012; Pinardi et al., 2014). However, at the sub-basin scale, the steric component can explain a substantial part of the total sea-level variance, for instance in the Aegean (68%), Southern Central Mediterranean (48%), and Levantine (42%), consistent with Mohamed and Skliris (2022). Regarding long-term trends, the steric component in the other sub-basins proved to be non-significant (Figures 3B, 5), as well as the halosteric component in the Aegean (Figures 3D, 5C), which is linked to the progressive presence of significant inflections with opposite signs along the time series, resulting in an irregular oscillation around zero through time. Furthermore, the weak contribution of the steric component to the total sea level is linked to the opposite evolution of the thermosteric (water expansion owing to increasing ocean temperature) and halosteric (water contraction owing to increasing salinity) effects (Figures 3C, D), which cancel each other out in almost all sub-basins.

Four main change points in the total sea-level trend arose from our analysis over 1993–2019 (Figure 2B), occurring around 1997, 2006, 2010, and 2016. These matched perfectly with the occurrence of NIG reversal episodes in the Ionian (von Schuckmann et al., 2019; Menna et al., 2022), where the surface circulation switched from anticyclonic to cyclonic (1997 and 2011) and vice-versa (2006 and 2017). These changes strongly impacted the water mass redistribution and thermohaline circulation throughout the EMed (Vigo et al., 2005; Gačić et al., 2010), thus affecting the sea level and generating a significant inflection in trends, as previously observed in 1998 (Vera et al., 2009). Generally, all sub-basins within the EMed move up and down in phases (Figure 4), leading to a breathing oscillation (Vigo et al., 2005), where the Ionian behaves the opposite way to the other sub-basins. This behavior can also be observed for the steric component, similar to the total sea level inflections. Accordingly, variations in the steric component seem to be the main cause of breathing oscillations observed in the total sea level, thus driving this variability at the sub-basin and Mediterranean Sea scales which emerge from quasi-decadal trend

changes. This is also supported by the 2016 inflection observations, where the bimodal breathing oscillation was not detected in the steric component, and therefore not in the total sea level. However, this inflection cannot be accurately assessed, both because the time series end in December 2019 and because a brief NIG shift that occurred around 2012 could have influenced the evolution of the phenomenon.

The contribution of the steric and non-steric components to the total sea level inflections change over time at the Mediterranean Sea scale. For example, in 1997, a negative inflection of -6.9 and -6.7 mm/yr was observed for the total sea level and steric component, respectively, then in 2006, positive inflections of 11 (total) and 5.5 (steric) mm/yr, whereas in 2010 negative inflections again of approximately -8.9 (total) and -1.6 (steric) mm/yr were observed. Unlike the previous events, the steric and non-steric effects in 2016 were found to contribute with opposing signs, with the steric component exhibiting a negative inflection of approximately -5.6 mm/yr and the non-steric component contributing positively (5.6 mm/yr) to the total sea level (as observed for the same type of NIG reversal in 2006). Some changes within the steric component properties were also observed for each reversal episode, with the thermosteric (halosteric) effect explaining approximately 97% (3%) of the steric variability in 1997, 69% (31%) in 2006, 68% (32%) in 2010, and 48% (52%) in 2016. Finally, the peak-to-peak amplitude of each breathing oscillation is consistent with each NIG reversal (ca. 9-10 cm), at least over the altimetric era, for the total sea level and steric component.

The residual contribution attributed to the non-steric effects increased over time, from approximately 2% in 1997 to 50% in 2006, 80% in 2010, and again 50% in 2016. Furthermore, the contribution of the halosteric effect has increased over time, balancing out the thermosteric contribution; this could have had an impact on the contribution of the steric component over time, as the contrast between thermosteric and halosteric effects gradually led to a cancellation of the steric variability. The 1997 inflection was strongly influenced by the steric and thermosteric effects, while a singular behavior can be observed in the EMed time series for this period (Figure 5). Therefore, it is possible that the concurrent effect of NIG reversal and EMT relaxation, which occurred around 1997, is the cause of the divergence of 1997 inflection and the subsequent inflections. However, EMT (as well as WMT) might be a non-recurrent phenomenon occurring at time scales longer than the decadal (Gačić et al., 2013; Roether et al., 2014), in contrast to NIG reversal episodes that appear to be cyclical at a quasi-decadal time scale (Gačić et al., 2010). The stronger contribution of the non-steric effects observed in 2010, instead, may be linked to an anomalously low NAO index that, in the winter of 2010, led to an average increase in the Mediterranean sea level of about 12 cm (Tsimplis et al., 2013). The extent of the phenomenon, however, was found to be variable among the sub-basins (see Bonaduce et al., 2016).

The individual thermosteric and halosteric effects allow the observation of the main variability occurring at the sub-basin scale, the main driver that modifies the steric component. Each breathing oscillation underlies variations in thermohaline properties and water mass redistribution at the sub-basin scale over the EMed owing to NIG reversal episodes. Switches to cyclonic NIG phases (1997, 2011) led to relative freshening and cooling of Levantine water while shifting to an anticyclonic phase (2006 and 2017) to salinization and warming, thereby impacting LIW properties in both cases. Changes in LIW properties are then reflected throughout the EMed sub-basins by flowing westward and changing the thermohaline properties of the intermediate depth layer. The thermosteric effect seems to be the main driver of the Levantine and Aegean steric variability. In contrast, the halosteric effect in the Adriatic and Southern Central Mediterranean contributes similarly to the steric variability of the Ionian, albeit influencing different portions of the sub-basin. The simultaneous opposite changes in both effects in some inflections led to annulment; thus, no significant steric inflections were generated in these cases. However, the steric inflection in the Adriatic, usually limited to the SAG area, cannot explain the significant inflections achieved from altimetry over the whole sub-basin. This suggests that the water mass redistribution, linked to the NIG, could be the dominant driver for this sub-basin, in which sea-level trends increase (decrease) during cyclonic (anticyclonic) phases due to the intake (lack) of AW flowing directly from the Sicily Channel.

The only significant inflection observed for total sea level in 2016 arose in the Western Mediterranean (Figure 5I), specifically in the EAG-Balearic Islands (Figure 4), where a positive jump was observed in altimetry, steric, and thermosteric trends. This variation is limited to the WMed and is probably linked to the WMT footprint, as it also occurred around 2004 over the same sub-basins (namely the Tyrrhenian and the Western Mediterranean).

This study highlights how non-linearity of sea-level trends within the Mediterranean Sea occurs due to oceanographic processes at the sub-basin scale, which is also reflected at the basin scale. Critical dynamic effects such as the NIG reversal phenomenon in the Ionian, which occurs at a quasi-decadal cyclicity, significantly affect the sea-level trends, especially in the EMed. This suggests that for the Mediterranean Sea, sea-level time series should be analyzed carefully, paying attention to both regionalization and to the fact that the processes acting in a given location reflect a chain of changes that have taken place elsewhere. Furthermore, sea-level projections in the Mediterranean Sea should take into account the existence of this non-linearity, which acts differentially between the sub-basins and significantly impacts the trend in the short and medium term. Future works should look further into the non-steric effects, in order to better understand which, and if, other processes could play an important role in driving the sea-level trend changes. Additionally, inflections on the steric component could also be evaluated separately for the surface and intermediate depths, thus better attributing sea-level trend changes to a specific process at the sub-basin scale.

Data availability statement

The raw data supporting the conclusions of this article will be made available by the authors, without undue reservation.

Author contributions

MO and MM contributed to conception and design of the study. CR supervised the work. CC performed the computation of the datasets. MM performed the analyses and wrote the first draft of the manuscript. AS, CC, CR, and MO contributed to manuscript revision. All authors contributed to the article and approved the submitted version.

Funding

This study has been partly developed in the framework of the MACMAP project funded by Istituto Nazionale di Geofisica e Vulcanologia (Environment Department), and partly by BiGeA funding, RFO project (CR).

Acknowledgments

The authors would like to thank Giorgio Spada, Marco Zavatarelli and Nadia Pinardi for their valuable suggestions on an earlier version of this paper. This work was carried out in the framework of the Ph.D. course in *Future Earth, Climate Change and Societal Challenges* (University of Bologna), and facilitated by a research visit to the NIOZ Royal Netherlands Institute of Sea Research (Yerseke, the Netherlands). The authors express their gratitude to Hazem Nagy and William Llovel whose valuable revisions significantly enhanced the quality of this work.

Conflict of interest

The authors declare that the research was conducted in the absence of any commercial or financial relationships that could be construed as a potential conflict of interest.

Publisher's note

All claims expressed in this article are solely those of the authors and do not necessarily represent those of their affiliated organizations, or those of the publisher, the editors and the reviewers. Any product that may be evaluated in this article, or claim that may be made by its manufacturer, is not guaranteed or endorsed by the publisher.

References

Argus, D. F., Peltier, W. R., Drummond, R., and Moore, A. W. (2014). The Antarctica component of postglacial rebound model ICE-6G_C (VM5a) based upon GPS positioning, exposure age dating of ice thickness, and relative sea level histories. *Geophys. J. Int.* 198, 537–563. doi: 10.1093/gji/ggu140

Artegiani, A., Paschini, E., Russo, A., Bregant, D., Raicich, F., and Pinardi, N. (1997). The Adriatic Sea general circulation. part II: Baroclinic circulation structure. *J. Phys. Oceanogr.* 27, 1515–1532. doi: 10.1175/1520-0485(1997)027<1515:TASGCP>2.0.CO;2

Ayoub, N., Le Traon, P.-Y., and De Mey, P. (1998). A description of the Mediterranean surface variable circulation from combined ERS-1 and TOPEX/POSEIDON altimetric data. *J. Mar. Syst.* 18, 3–40. doi: 10.1016/S0924-7963(98)80004-3

Beckley, B. D., Callahan, P. S., Hancock, D. W., Mitchum, G. T., and Ray, R. D. (2017). On the "cal-mode" correction to TOPEX satellite altimetry and its effect on the global mean sea level time series. *J. Geophys. Res.: Oceans* 122, 8371–8384. doi: 10.1002/2017JC013090

Bensi, M., Cardin, V., Rubino, A., Notarstefano, G., and Poulain, P. M. (2013). Effects of winter convection on the deep layer of the southern Adriatic Sea in 2012. *J. Geophys. Res. Oceans* 118, 6064–6075. doi: 10.1002/2013JC009432

Beranger, K., Mortier, L., Gasparini, G. P., Gervasio, L., Astraldi, M., and Crepon, M. (2004). The dynamics of the Sicily strait: a comprehensive study from observations and models. *Deep Sea Res. Part II: Topical Stud. Oceanogr.* 51, 411–440. doi: 10.1016/j.dsr2.2003.08.004

Bessières, L., Rio, M. H., Dufau, C., Boone, C., and Pujol, M. I. (2013). Ocean state indicators from MyOcean altimeter products. *Ocean Sci.* 9, 545–560. doi: 10.5194/os-9-545-2013

Bonaduce, A., Pinardi, N., Oddo, P., Spada, G., and Larnicol, G. (2016). Sea-Level variability in the Mediterranean Sea from altimetry and tide gauges. *Clim. Dyn.* 47, 2851–2866. doi: 10.1007/s00382-016-3001-2

Borzelli, G. L. E., Gačić, M., Cardin, V., and Civitarese, G. (2009). Eastern Mediterranean Transient and reversal of the Ionian Sea circulation. *Geophys. Res. Lett.* 36, L15108. doi: 10.1029/2009GL039261

C3S Copernicus Climate change service. In: *Satellite altimetry data*. Available at: https://climate.copernicus.eu/ (Accessed Aug 19, 2022).

Calafat, F. M., Chambers, D. P., and Tsimplis, M. N. (2012). Mechanism of decadal sea level variability in the eastern north Atlantic and the Mediterranean Sea. *J. Geophys. Res.* 117, C09022. doi: 10.1029/2012JC008285

Calafat, F. M., Frederikse, T., and Horsburgh, K. (2022). The sources of Sea-level changes in the Mediterranean Sea since 1960. *J. Geophys. Res. Oceans* 127, e2022JC019061. doi: 10.1029/2022JC019061

Calafat, F. M., Marcos, M., and Gomis, D. (2010). Mass contribution to the Mediterranean Sea level variability for the period 1948-2000. *Glob. Planet. Change* 73, 193–201. doi: 10.1016/j.gloplacha.2010.06.002

Camargo, C. M. L., Riva, R. E. M., Hermans, T. H. J., and Slangen, A. B. A. (2020). Exploring sources of uncertainty in steric Sea-level change estimates. *J. Geophys. Res. Oceans* 125, 1–18. doi: 10.1029/2020JC016551

Carillo, A., Sannino, G., Artale, V., Ruti, P., Calmanti, S., and Dell'Aquila, A. (2012). Steric sea level rise over the Mediterranean Sea: present climate and scenario simulations. *Clim. Dyn.* 39, 2167–2184. doi: 10.1007/s00382-012-1369-1

Cazenave, A., Bonnefond, P., Mercier, F., Dominh, K., and Toumazou, V. (2002). Sea Level variations in the Mediterranean Sea and black Sea from satellite altimetry and tide gauges. *Glob. Planet. Change* 34, 59–86. doi: 10.1016/S0921-8181(02)00106-6

Cazenave, A., Cabanes, C., Dominh, K., and Mangiarotti, S. (2001). Recent sea level change in the Mediterranean Sea revealed by Topex/Poseidon satellite altimetry. *Geophys. Res. Lett.* 28, 1607–1610. doi: 10.1029/2000GL012628

Chiggiato, J., Artale, V., Durrieu de Madron, X., Schroeder, K., Taupier-Letage, I., Velaoras, D., et al. (2023). "Chapter 9 - Recent changes in the Mediterranean Sea," in *Oceanography of the Mediterranean Sea*. Eds. K. Schroeder and J. Chiggiato (Elsevier), 289–334. doi: 10.1016/B978-0-12-823692-5.00008-X

Cho, H., and Fryzlewicz, P. (2015). Multiple-change-point detection for high dimensional time series *via* sparsified binary segmentation. *J. R. Stat. Soc. Ser. B* 77, 475–507. doi: 10.1111/rssb.12079

Chow, G. C. (1960). Tests of equality between sets of coefficients in two linear regressions. *Econometrica* 28, 591–605. doi: 10.2307/1910133

Civitarese, G., Gačić, M., Eusebi Borzelli, G. L., and Lipizer, M. (2010). On the impact of the bimodal oscillating system (BiOS) on the biogeochemistry and biology of the Adriatic and Ionian seas (eastern Mediterranean). *Biogeosciences* 7, 3987–3997. doi: 10.5194/bg-7-3987-2010

CMEMS Copernicus Marine service. In: *Mediterranean Reanalysis dataset*. Available at: https://marine.copernicus.eu/ (Accessed Aug 19, 2022).

Criado-Aldeanueva, F., and Soto-Navarro, J. (2020). Climatic indices over the Mediterranean Sea: A review. *Appl. Sci.* 10, 5790. doi: 10.3390/app10175790

Demirov, E., and Pinardi, N. (2002). Simulation of the Mediterranean circulation from 1979 to 1993 model simulations: Part II. energetics of variability. *J. Mar. Syst.* 33, 23–50. doi: 10.1016/S0924-7963(02)00051-9

Dieng, H. B., Cazenave, A., Meyssignac, B., and Ablain, M. (2017). New estimate of the current rate of sea level rise from a sea level budget approach. *Geophys. Res. Lett.* 44, 3744–3751. doi: 10.1002/2017GL073308

Dobricic, S., and Pinardi, N. (2008). An oceanographic three-dimensional variational data assimilation scheme. *Ocean Model.* 22, 89–105. doi: 10.1016/j.ocemod.2008.01.004

Escudier, R., Clementi, E., Cipollone, A., Pistoia, J., Drudi, M., Grandi, A., et al. (2021). A high resolution reanalysis for the Mediterranean Sea. *Front. In Earth Sci.* 9. doi: 10.3389/feart.2021.702285

Escudier, R., Clementi, E., Omar, M., Cipollone, A., Pistoia, J., Aydogdu, A., et al. (2020). Mediterranean Sea Physical reanalysis (CMEMS MED-currents) (Version 1) *Data set*. *Copernicus Monit. Environ. Mar. Service (CMEMS)*. doi: 10.25423/CMCC/MEDSEA_MULTIYEAR_PHY_006_004_E3R1

Fenoglio-Marc, L. (2002). Long-term sea level change in the Mediterranean Sea from multi-satellite altimetry and tide gauges. *Phys. Chem. Earth* 27, 1419–1431. doi: 10.1016/S1474-7065(02)00084-0

Fox-Kemper, B., Hewitt, H. T., Xiao, C., Aðalgeirsdóttir, G., Drijfhout, S. S., Edwards, T. L., et al. (2021). "Ocean, cryosphere and Sea level change," in *Climate change 2021: The physical science basis. contribution of working group I to the sixth assessment report of the intergovernmental panel on climate change*. Eds. V. Masson-Delmotte, P. Zhai, A. Pirani, S. L. Connors, C. Péan, S. Berger, N. Caud, Y. Chen, L. Goldfarb, M. I. Gomis, M. Huang, K. Leitzell, E. Lonnoy, J. B. R. Matthews, T. K. Maycock, T. Waterfield, O. Yelekçi, R. Yu and B. Zhou (Cambridge, United Kingdom and New York, NY, USA: Cambridge University Press), 1211–1362. doi: 10.1017/9781009157896.011

Gačić, M., Civitarese, G., Eusebi Borzelli, G. L., Kovačević, V., Poulain, P.-M., Theocharis, A., et al. (2011). On the relationship between the decadal oscillations of the northern Ionian Sea and the salinity distributions in the Eastern Mediterranean. *J. Geophys. Res.* 116, C12002. doi: 10.1029/2011JC007280

Gačić, M., Civitarese, G., Kovačević, V., Ursella, L., Bensi, M., Menna, M., et al. (2014). Extreme winter 2012 in the Adriatic: an example of climatic effect on the BiOS rhythm. *Ocean Sci.* 10, 513–522. doi: 10.5194/os-10-513-2014

Gačić, M., Eusebi Borzelli, G. L., Civitarese, G., Cardin, V., and Yari, S. (2010). Can internal processes sustain reversal of the ocean upper circulation? the Ionian Sea example. *Geophys. Res. Lett.* 37. doi: 10.1029/2010GL043216

Gačić, M., Schroeder, K., Civitarese, G., Cosoli, S., Vetrano, A., and Eusebi Borzelli, G. L. (2013). Salinity in the Sicily channel corroborates the role of the Adriatic-Ionian bimodal oscillating system (BiOS) in shaping the decadal variability of the Mediterranean overturning circulation. *Ocean Sci.* 9, 83–90. doi: 10.5194/os-9-83-2013

Galassi, G., and Spada, G. (2014). Sea-Level rise in the Mediterranean Sea by 2050: Roles of terrestrial ice melt, steric effects and glacial isostatic adjustment. *Glob. Planet. Change* 123, 55–66. doi: 10.1016/j.gloplacha.2014.10.007

Gambolati, G., and Teatini, P. (1998). "Numerical analysis of land subsidence due to natural compaction of the upper Adriatic Sea basin," in *CENAS, coastline evolution of the upper Adriatic Sea due to Sea level rise and natural and anthropogenic land subsidence*, vol. 28 . Ed. G. Gambolati (Norwell, MA, USA: Kluwer Academic Publishing, Water Science & Technology Library), 103–131.

García, D., Vigo, I., Chao, B. F., and Martínez, M. C. (2007). Vertical crustal motion along the Mediterranean and black Sea coast derived from ocean altimetry and tide gauge data. *Pure Appl. Geophys.* 164, 851–863. doi: 10.1007/s00024-007-0193-8

Gill, A. E., and Niller, P. P. (1973). The theory of the seasonal variability in the ocean. *Deep Sea Res. Oceanogr. Abstract* 20, 141–177. doi: 10.1016/0011-7471(73)90049-1

Giorgi, F. (2006). Climate change hot-spots. *Geophys. Res. Lett.* 33, L08707. doi: 10.1029/2006GL025734

Golnaraghi, M., and Robinson, A. R. (1994). "Dynamical studies of the Eastern Mediterranean circulation," in *Ocean processes in climate dynamics: Global and Mediterranean examples, NATO science series c*, vol. 419 . Eds. P. Malanotte-Rizzoli and A. R. Robinson (Springer, Dordrecht: Kluwer Academic Publishers), 437.

Grodsky, S. A., Reul, N., Bentamy, A., Vandemark, D., and Guimbard, S. (2019). Eastern Mediterranean Salinification observed in satellite salinity from SMAP mission. *J. Mar. Syst.* 198, 103190. doi: 10.1016/j.jmarsys.2019.103190

Hamed, K. H., and Rao, A. R. (1998). A modified Mann-Kendall trend test for autocorrelated data. *J. Hydrol.* 204, 182–196. doi: 10.1016/S0022-1694(97)00125-X

Harchaoui, Z., and Cappé, O. (2007). "Retrospective mutiple change-point estimation with kernels," in *IEEE/SP 14th workshop on statistical signal processing*, vol. 2007. (Madison, WI, USA: IEEE), 768–772. doi: 10.1109/SSP.2007.4301363

Heburn, G. W., and La Violette, P. E. (1990). Variations in the structure of the anticyclonic gyres found in the alboran Sea. *J. Geophys. Res.* 95, 1599–1613. doi: 10.1029/JC095iC02p01599

Hecht, A., Pinardi, N., and Robinson, A. R. (1988). Currents, water masses, eddies and jets in the Mediterranean levantine basin. *J. Phys. Oceanogr.* 18, 1320–1353. doi: 10.1175/1520-0485(1988)018<1320:CWMEAJ>2.0.CO;2

Iona, A., Theodorou, A., Sofianos, S., Watelet, S., Troupin, C., and Beckers, J. M. (2018). Mediterranean Sea climatic indices: Monitoring long-term variability and climate changes. *Earth Syst. Sci. Data* 10, 1829–1842. doi: 10.5194/essd-10-1829-2018

IPCC (2021). "Climate change 2021," in *The physical science basis. contribution of working group I to the sixth assessment report of the intergovernmental panel on climate change*. Eds. V. Masson-Delmotte, P. Zhai, A. Pirani, S. L. Connors, C. Péan, S. Berger, N. Caud, Y. Chen, L. Goldfarb, M. I. Gomis, M. Huang, K. Leitzell, E. Lonnoy, J. B. R. Matthews, T. K. Maycock, T. Waterfield, O. Yelekçi, R. Yu and X. X. X. B. Zhou (Cambridge, United Kingdom and New York, NY, USA: Cambridge University Press). doi: 10.1017/9781009157896

Jones, P. W. (1999). First- and second-order conservative remapping schemes for grids in spherical coordinates. *Monthly Weather Rev.* 127, 2204–2210. doi: 10.1175/1520-0493(1999)127<2204:FASOCR>2.0.CO;2

Jevrejeva, S., Moore, J. C., Grinsted, A., Matthews, A. P., and Spada, G. (2014). Trends and acceleration in global and regional sea levels since 1807. *Glob. Planet. Change* 113, 11–22. doi: 10.1016/j.gloplacha.2013.12.004

Kendall, M. G. (1975). *Rank correlation methods. 4th ed.* Ed. C. Griffin (London, UK: Charles Griffin).

Killick, R., Fearnhead, P., and Eckley, I. (2012). Optimal detection of changepoints with a linear computational cost. *J. Amer. Stat. Assoc.* 107, 1590–1598. doi: 10.1080/01621459.2012.737745

Korres, G., Pinardi, N., and Lascaratos, A. (2000). The ocean response to low frequency inter-annual atmospheric variability in the Mediterranean sea. part, i. sensitivity experiments and energy analysis. *J. Clim.* 13, 705–731. doi: 10.1175/1520-0442(2000)013<0705:TORTLF>2.0.CO;2

Kourafalou, V. H., and Barbopoulos, K. (2003). High resolution simulations on the north Aegean Sea seasonal circulation. *Ann. Geophys.* 21, 251–265. doi: 10.5194/angeo-21-251-2003

Landerer, F. W., and Volkov, D. L. (2013). The anatomy of recent large sea level fluctuations in the Mediterranean Sea. *Geophys. Res. Lett.* 40, 553–557. doi: 10.1002/grl.50140

Larnicol, G., Ayoub, N., and Le Traon, P. Y. (2002). Major changes in Mediterranean Sea level variability from 7 years of TOPEX/Poseidon and ERS-1/2 data. *J. Mar. Syst.* 33–34, 63–89. doi: 10.1016/S0924-7963(02)00053-2

Lascaratos, A., Williams, R. G., and Tragou, E. (1993). A mixed-layer study of the formation of levantine intermediate water. *J. Geophys. Res.* 98, 14739–14749. doi: 10.1029/93JC00912

Legeais, J., Meyssignac, B., Faugère, Y., Guerou, A., Ablain, M., Pujol, M.-I., et al. (2021). Copernicus Sea Level space observations: A basis for assessing mitigation and developing adaptation strategies to Sea level rise. *Front. Mar. Sci.* 8. doi: 10.3389/fmars.2021.704721

Lermusiaux, P., and Robinson, A. (2001). Features of dominant mesoscale variability, circulation patterns and dynamics in the strait of Sicily. *Deep Sea Res. Part I: Oceanogr. Res. Pap.* 48, 1953–1997. doi: 10.1016/S0967-0637(00)00114-X

Levitus, S., Antonov, J. I., Boyer, T. P., Baranova, O. K., Garcia, H. E., Locarnini, R. A., et al. (2012). World ocean heat content and thermosteric sea level change (0–2000 m), 1955–2010. *Geophys. Res. Lett.* 39, L10603. doi: 10.1029/2012GL051106

Madec, G., Bourdallé-Badie, R., Bouttier, P.-A., Bricaud, C., Bruciaferri, D., Calvert, D., et al. (2017). *NEMO ocean engine* (Paris, France: Notes du Pôle de modélisation de l \'Institut Pierre-Simon Laplace (IPSL). doi: 10.5281/zenodo.1472492

Madec, G., Delecluse, P., Crepon, M., and Chartier, M. (1991). A three-dimensional numerical study of deep-water formation in the northwestern Mediterranean Sea. *J. Phys. Oceanogr.* 21, 1349–1371. doi: 10.1175/1520-0485(1991)021<1349:ATDNSO>2.0.CO;2

Malanotte-Rizzoli, P., Manca, B. B., D'Alcalà, R., Theocharis, A., Bergamasco, A., Bregant, D., et al. (1997). A synthesis of the Ionian Sea hydrography, circulation and water mass pathways during POEM-phase I. *Prog. Oceanogr.* 39, 153–204. doi: 10.1016/S0079-6611(97)00013-X

Malanotte-Rizzoli, P., Manca, B. B., Ribera d'Alcalà, M., Theocharis, A., Brenner, S., Budillon, G., et al. (1999). The eastern Mediterranean in the 80s and in the 90s: The big transition in the intermediate and deep circulations. *Dyn. Atmos. Oceans* 29, 365–395. doi: 10.1016/S0377-0265(99)00011-1

Manca, B. B. (2000). "Recent changes in dynamics of the eastern Mediterranean affecting the water characteristics of the adjacent basins," in *The Eastern Mediterranean climatic transient: Its origin, evolution and impact on the ecosystem*, vol. 10 . Ed. F. Briand (Monaco: CIESM Workshop Ser.), 27–31. Mediter. Sci. Comm., Monaco.

Manca, B. B., Budillon, G., Scarazzato, P., and Ursella, L. (2003). Evolution of dynamics in the eastern Mediterranean affecting water mass structures and properties in the Ionian and Adriatic seas. *J. Geophys. Res. Oceans* 108, 8102. doi: 10.1029/2002JC001664

Mann, H. B. (1945). Non-parametric tests against trend. *Econometrica* 13, 163–171. doi: 10.2307/1907187

Mariotti, A., and Dell'Aquila, A. (2012). Decadal climate variability in the Mediterranean region: Roles of large-scale forcings and regional processes. *Clim. Dyn.* 38, 1129–1145. doi: 10.1007/s00382-011-1056-7

Marullo, S., Artale, V., and Santoleri, R. (2011). The SST multidecadal variability in the Atlantic-Mediterranean region and its relation to AMO. *J. Climate* 24, 4385–4401. doi: 10.1175/2011JCLI3884.1

Mauri, E., Sitz, L., Gerin, R., Poulain, P.-M., Hayes, D., and Gildor, H. (2019). On the variability of the circulation and water mass properties in the Eastern levantine Sea between September 2016–august 2017. *Water* 11, 1741. doi: 10.3390/w11091741

McDougall, T. J., and Barker, P. M. (2011) *Getting started with TEOS-10 and the Gibbs seawater oceanographic toolbox*. Available at: http://www.teos-10.org/pubs/Getting_Started.pdf.

McDougall, T. J., Jackett, D. R., Millero, F. J., Pawlowicz, R., and Barker, P. M. (2012). A global algorithm for estimating absolute salinity. *Ocean Sci.* 8, 1123–1134. doi: 10.5194/os-8-1123-2012

Meli, M., Olivieri, M., and Romagnoli, C. (2021). Sea-Level change along the Emilia-romagna coast from tide gauge and satellite altimetry. *Remote Sens.* 13, 97. doi: 10.3390/rs13010097

Meli, M., and Romagnoli, C. (2022). Evidence and implications of hydrological and climatic change in the Reno and lamone river basins and related coastal areas (Emilia-romagna, northern Italy) over the last century. *Water* 14, 2650. doi: 10.3390/w14172650

Melini, D., and Spada, G. (2019). Some remarks on glacial isostatic adjustment modelling uncertainties. *Geophys. J. Int.* 218, 401–413. doi: 10.1093/gji/ggz158

Menemenlis, D., Fukumori, I., and Lee, T. (2007). Atlantic To Mediterranean Sea level difference driven by winds near Gibraltar strait. *J. Phys. Oceanogr.* 37, 359–376. doi: 10.1175/JPO3015.1

Menna, M., Gačić, M., Martellucci, R., Notarstefano, G., Fedele, G., Mauri, E., et al. (2022). Climatic, decadal, and interannual variability in the upper layer of the Mediterranean Sea using remotely sensed and in-situ data. *Remote Sens.* 14, 1322. doi: 10.3390/rs14061322

Menna, M., Gerin, R., Notarstefano, G., Mauri, E., Bussani, A., Pacciaroni, M., et al. (2021). On the circulation and thermohaline properties of the Eastern Mediterranean Sea. *Front. Mar. Sci.* 8. doi: 10.3389/fmars.2021.671469

Menna, M., Poulain, P.-M., Zodiatis, G., and Gertman, I. (2012). On the surface circulation of the levantine sub-basin derived from Lagrangian drifters and satellite altimetry data. *Deep-Sea Res. Part I* 65, 46–58. doi: 10.1016/j.dsr.2012.02.008

Menna, M., Reyes-Suarez, N. C., Civitarese, G., Gačić, M., Poulain, P.-M., and Rubino, A. (2019). Decadal variations of circulation in the central Mediterranean and its interactions with the mesoscale gyres. *Deep Sea Res. Part II Top. Stud. Oceanogr.* 164, 14–24. doi: 10.1016/j.dsr2.2019.02.004

Mihanović, H., Vilibić, I., Carniel, S., Tudor, M., Russo, A., Bergamasco, A., et al. (2013). Exceptional dense water formation on the Adriatic shelf in the winter of 2012. *Ocean Sci.* 9, 561–572. doi: 10.5194/os-9-561-2013

Milliff, R. F., and Robinson, A. R. (1992). Structure and dynamics of the rhodes gyre system and dynamical interpolation for estimates of the mesoscale variability. *J. Phys. Oceanogr.* 22, 317–337. doi: 10.1175/1520-0485(1992)022<0317:SADOTR>2.0.CO;2

Millot, C. (1985). Some features of the Algerian current. *J. Geophys. Res.* 90, 7169–7176. doi: 10.1029/JC090iC04p07169

Miramontes, E., Déverchère, J., Pellegrini, C., and Chiarella, D. (2022). "Mediterranean Sea Evolution and present-day physiography," in *Oceanography of the Mediterranean Sea*. Eds. K. Schroeder and J. Chiggiato (Elsevier), 13–39.

Mohamed, B., Abdallah, A. M., Alam El-Din, K., Nagy, H., and Shaltout, M. (2019a). Inter-annual variability and trends of Sea level and Sea surface temperature in the Mediterranean Sea over the last 25 years. *Pure Appl. Geophys.* 176, 3787–3810. doi: 10.1007/s00024-019-02156-w

Mohamed, B., Mohamed, A., Alam El-Din, K., Nagy, H., and Elsherbiny, A. (2019b). Sea Level changes and vertical land motion from altimetry and tide gauges in the southern levantine basin. *J. Geodyn.* 128, 1–10. doi: 10.1016/j.jog.2019.05.007

Mohamed, B., and Skliris, N. (2022). Steric and atmospheric contributions to interannual sea level variability in the eastern Mediterranean sea over 1993-2019. *Oceanologia* 64, 50–62. doi: 10.1016/j.oceano.2021.09.001

Nagy, H., Di-Lorenzo, E., and El-Gindy, A. (2019). The impact of climate change on circulation patterns in the Eastern Mediterranean Sea upper layer using med-ROMS model. *Prog. Oceanogr.* 175, 226–244. doi: 10.1016/j.pocean.2019.04.012

Naranjo, C., García-Lafuente, J., Sammartino, S., Sánchez-Garrido, J. C., Sánchez-Leal, R. , and Jesús Bellanco, M. (2017). Recent changes, (2004-2016) of temperature and salinity in the Mediterranean outflow. *Geophys. Res. Lett.* 44, 5665–5672. doi: 10.1002/2017GL072615

Olivieri, M., and Spada, G. (2013). Intermittent sea-level acceleration. *Glob. Planet. Change* 109, 64–72. doi: 10.1016/j.gloplacha.2013.08.004

Onken, R., Robinson, A. R., Lermusiaux, P. F. J., Haley, P. J., and Anderson, L. A. (2003). Data-driven simulations of synoptic circulation and transports in the Tunisia-Sardinia-Sicily region. *J. Geophys. Res.: Oceans* 108, 8123. doi: 10.1029/2002JC001348

Passaro, M., and Seitz, F. (2010). Steric sea level variations in the central-eastern Mediterranean Sea from argo observations. *Bollettino di Geofisica Teorica Applicata* 52, 131–147.

Pastor, F., Valiente, J. A. , and Palau, J. L. (2018). Sea Surface temperature in the Mediterranean: Trends and spatial patterns, (1982–2016). *Pure Appl. Geophys.* 175, 4017–4029. doi: 10.1007/s00024-017-1739-z

Peltier, W. R., Argus, D. F., and Drummond, R. (2015). Space geodesy constrains ice age terminal deglaciation: The global ICE-6G-C (VM5a) model. *J. Geophys. Res. Solid Earth* 120, 450–487. doi: 10.1002/2014JB011176

Pinardi, N., Bonaduce, A., Navarra, A., Dobricic, S., and Oddo, P. (2014). The mean Sea level equation and its application to the Mediterranean Sea. *J. Clim.* 27, 442–447. doi: 10.1175/JCLI-D-13-00139.1

Pinardi, N., Korres, G., Lascaratos, A., Roussenov, V., and Stanev, E. (1997). Numerical simulation of the interannual variability of the Mediterranean Sea upper ocean circulation. *Geophys. Res. Lett.* 24, 425–428. doi: 10.1029/96GL03952

Pinardi, N., and Masetti, E. (2000). Variability of the large scale general circulation of the Mediterranean Sea from observations and modelling: a review. *Palaeogeogr. Palaeoclimatol. Palaeoecol.* 158, 153–173. doi: 10.1016/S0031-0182(00)00048-1

Pinardi, N., Zavatarelli, M., Adani, M., Coppini, G., Fratianni, C., Oddo, P., et al. (2015). Mediterranean Sea Large-scale low-frequency ocean variability and water mass formation rates from 1987 to 2007: A retrospective analysis. *Prog. Oceanogr.* 132, 318–332. doi: 10.1016/j.pocean.2013.11.003

Pinardi, N., Zavatarelli, M., Arneri, E., Crise, A., and Ravaioli, M. (2006). "The physical, sedimentary and ecological structure and variability of shelf areas in the Mediterranean Sea," in *THE GLOBAL the global coastal ocean: Interdisciplinary regional studies and syntheses*, vol. 14 . Eds. A. Robinson and K. Brink (Cambridge, MA, USA: Harvard University Press, The Sea). (Chapter 32).

Pinardi, N., Estournel, C., Cessi, P., Escudier, R., and Lyubartsev, V. (2023). "Chapter 7 - dense and deep water formation processes and Mediterranean overturning circulationOceanography of the Mediterranean Sea,". Eds. K. Schroeder and J. Chiggiato (Elsevier), 209–261. doi: 10.1016/B978-0-12-823692-5.00009-1

Pisacane, G., Artale, V., Calmanti, S., and Rupolo, V. (2006). Decadal oscillations in the Mediterranean Sea: a result of the overturning circulation variability in the eastern basin? *Clim. Res.* 31, 257–271. doi: 10.3354/cr031257

Pisano, A., Marullo, S., Artale, V., Falcini, F., Yang, C., Leonelli, F. E., et al. (2020). New evidence of Mediterranean climate change and variability from Sea surface temperature observations. *Remote Sens.* 12, 132. doi: 10.3390/rs12010132

Poulain, P. M., Centurioni, L., Özgökmen, T., Tarry, D., Pascual, A., Ruiz, S., et al. (2021). On the structure and kinematics of an Algerian eddy in the southwestern Mediterranean Sea. *Remote Sens.* 13, 3039. doi: 10.3390/rs13153039

Poulain, P.-M., Menna, M., and Mauri, E. (2012). Surface geostrophic circulation of the Mediterranean Sea derived from drifter and satellite altimeter data. *J. Phys. Oceanogr.* 42, 973–990. doi: 10.1175/JPO-D-11-0159.1

Puillat, I., Sorgente, R., Ribotti, A., Natale, S., and Echevin, V. (2006). Westward Branching of LIW induced by Algerian anticyclonic eddies close to the sardinian slope. *Chem. Ecol.* 22, S293–S305. doi: 10.1080/02757540600670760

Reale, M., Crise, A., Farneti, R., and Mosetti, R. (2016). A process study of the Adriatic-Ionian system baroclinic dynamics. *J. Geophys. Res. Oceans* 121, 5872–5887. doi: 10.1002/2016JC011763

Reale, M., Salon, S., Crise, A., Farneti, R., Mosetti, R., and Sannino, G. (2017). Unexpected covariant behavior of the Aegean and Ionian seas in the period 1987-2008 by means of a nondimensional Sea surface height index. *J. Geophys. Res. Oceans* 122, 8020–8033. doi: 10.1002/2017JC012983

Rice, G., and Zhang, C. (2022). Consistency of binary segmentation for multiple change-point estimation with functional data. *Stat Probability Lett.* 180, 109228. doi: 10.1016/j.spl.2021.109228

Robinson, A. R., Malanotte-Rizzoli, P., Hecht, A., Michelato, A., Roether, W., Theocharis, A., et al. (1992). General circulation of the Eastern Mediterranean. *Earth-Science Rev.* 32, 285–309. doi: 10.1016/0012-8252(92)90002-B

Robinson, A. R., Golnaraghi, M., Leslie, W. G., Artegiani, A., Hecht, A., Lazzoni, E., et al. (1991). The eastern Mediterranean general circulation: features, structure and variability. *Dynamics Atmospheres Oceans* 15, 215–240. doi: 10.1016/0377-0265(91)90021-7

Robinson, A. R., Leslie, W. G., Theocharis, A., and Lscaratos, A. (2001). "Mediterranean Sea Circulation," in *Encyclopedia of ocean sciences*. Ed. J. H. Steele (Academic Press), 1689–1705. doi: 10.1006/rwos.2001.0376

Robinson, A. R., Sellschopp, J., Warn-Varnas, A., Leslie, W. G., Lozano, C. J., Haley, P. J.Jr., et al. (1999). The Atlantic Ionian stream. *J. Mar. Syst.* 20, 129–156. doi: 10.1016/S0924-7963(98)00079-7

Roether, W., Klein, B., and Hainbucher, D. (2014). "The Eastern Mediterranean transient: Evidence for similar events previously? in geophysical monograph series, 202, AGU (American geophysical union)," in *The Mediterranean Sea: Temporal variability and spatial patterns* (Washington, USA: Wiley), 75–83. doi: 10.1002/9781118847572.ch6

Roether, W., Manca, B. B., Klein, B., Bregant, D., Georgopoulos, D., Beitzel, V., et al. (1996). Recent changes in eastern Mediterranean deep waters. *Science* 271, 333–335. doi: 10.1126/science.271.5247.333

Romagnoli, C., Bosman, A., Casalbore, D., Anzidei, M., Doumaz, F., Bonaventura, F., et al. (2022). Coastal erosion and flooding threaten low-lying coastal tracts at lipari (Aeolian islands, Italy). *Remote Sens.* 14, 2960. doi: 10.3390/rs14132960

Romanou, A., Tselioudis, G., Zerefos, C. S., Clayson, C.-A. J., Curry, A., and Andersson, A. (2010). Evaporation-precipitation variability over the Mediterranean and the black seas from satellite and reanalysis estimates. *J. Clim.* 23, 5268–5287. doi: 10.1175/2010JCLI3525.1

Schroeder, K., Chiggiato, J., Bryden, H. L., Borghini, M., and Ismail, S. B. (2016). Abrupt climate shift in the western Mediterranean Sea. *Sci. Rep.* 6, 23009. doi: 10.1038/srep23009

Schroeder, K., Chiggiato, J., Josey, S. A., Borghini, M., Aracri, S., and Sparnocchia, S. (2017). Rapid response to climate change in a marginal sea. *Sci. Rep.* 7, 4065. doi: 10.1038/s41598-017-04455-5

Schroeder, K., Josey, S. A., Herrmann, M., Grignon, L., Gasparini, G. P., and Bryden, H. L. (2010). Abrupt warming and salting of the Western Mediterranean deep water after 2005: Atmospheric forcings and lateral advection. *J. Geophys. Res.* 115, C08029. doi: 10.1029/2009JC005749

Scott, A. J., and Knott, M. (1974). A cluster analysis method for grouping means in the analysis of variance. *Biometrics* 30, 507–512. doi: 10.2307/2529204

Sen, P. K. (1968). Estimates of the regression coefficient based on kendall's tau. *J. Am. Stat. Assoc.* 63, 1379–1389. doi: 10.1080/01621459.1968.10480934

Sen, A., and Srivastava, M. S. (1975). On tests for detecting change in mean. *Ann. Stat* 3, 98–108. doi: 10.1214/aos/1176343001

Skliris, N., Zika, J. D., Herold, L., Josey, S. A., and Marsh, R. (2018). Mediterranean Sea water budget long-term trend inferred from salinity observations. *Clim. Dyn.* 51, 2857–2876. doi: 10.1007/s00382-017-4053-7

Slangen, A. B. A., van de Wal, R. S. W., Wada, Y. , and Vermeersen, L. L. A. (2014). Comparing tide gauge observations to regional patterns of sea-level change, (1961-2003). *Earth Syst. Dynam.* 5, 243–255. doi: 10.5194/esd-5-243-2014

Sparnocchia, S., Gasparini, G. P., Astraldi, M., Borghini, M., and Pistek, P. (1999). Dynamics and mixing of the Eastern Mediterranean outflow in the tyrrhenian basin. *J. Mar. Syst.* 20, 301–317. doi: 10.1016/S0924-7963(98)00088-8

Stammer, D., Cazenave, A., Ponte, R. M., and Tamisiea, M. E. (2013). "Causes for contemporary regional sea level changes," in *Annual review of marine science, annual reviews*, vol. 5 . Eds. C. A. Carlson and S. J. Giovannoni (CA, USA: Palo Alto), 21–46.

Storto, A., Bonaduce, A., Feng, X., and Yang, C. (2019). Steric sea level changes from ocean reanalyses at global and regional scales. *Water* 11, 1987. doi: 10.3390/w11101987

Syvitski, J., Kettner, A., Overeem, I., Hutton, E., Hannon, M., Brakenridge, G. R., et al. (2009). Sinking deltas due to human activities. *Nat. Geosci.* 2, 681–686. doi: 10.1038/ngeo629

Taburet, G., Sanchez-Roman, A., Ballarotta, M., Pujol, M.-I., Legeais, J.-F., Fournier, F., et al. (2019). DUACS DT2018: 25 years of reprocessed sea level altimetry products. *Ocean Sci.* 15, 1207–1224. doi: 10.5194/os-15-1207-2019

Tanhua, T., Hainbucher, D., Schroeder, K., Cardin, V., Álvarez, M., and Civitarese, G. (2013). The Mediterranean Sea system: a review and an introduction to the special issue. *Ocean Sci.* 9, 789–803. doi: 10.5194/os-9-789-2013

Theil, H. (1950). *A rank-invariant method of linear and polynomial regression analysis* Vol. 1950 (Berlin/Heidelberg, Germany: Nederl. Akad. Wetensch., Proc. Springer).

Theocharis, A., Nittis, K., Kontoyiannis, H., Papageoirgiou, E., and Balopoulos, E. (1999). Climatic changes in the Aegean Sea influence the eastern Mediterranean thermohaline circulation, (1986–1997). *Geophys. Res. Lett.* 26, 1617–1620. doi: 10.1029/1999GL900320

Theocharis, A., Krokos, G., Velaoras, D., and Korres, G. (2014). An internal mechanism driving the alternation of the eastern mediterranean dense/deep water sources. *Mediterr. Sea: Temporal Variab. Spatial Patterns* 113–137. doi: 10.1002/9781118847572.ch8

Tomczak, M., and Godfrey, J. S. (2003). "Temperature, salinity, density and oceanic pressure field," in *Regional oceanography: An introduction* (Delhi: Daya Publishing House), 15–28.

Truong, C., Oudre, L., and Vayatis, N. (2020). Selective review of offline change point detection methods. *Signal Process.* 167, 107299. doi: 10.1016/j.sigpro.2019.107299

Tsimplis, M. N., and Baker, T. F. (2000). Sea Level drop in the Mediterranean Sea: An indicator of deep water salinity and temperature changes? *Geophys. Res. Lett.* 27, 1731–1734. doi: 10.1029/1999GL007004

Tsimplis, M. N., Calafat, F. M., Marcos, M., Jordà, G., Gomis, D., Fenoglio-Marc, L., et al. (2013). The effect of the NAO on sea level and on mass changes in the Mediterranean Sea. *J. Geophys. Res. Oceans* 118, 944–952. doi: 10.1002/jgrc.20078

Tsimplis, M. N., and Josey, S. A. (2001). Forcing of the Mediterranean Sea by atmospheric oscillations over the north Atlantic. *Geophys. Res. Lett.* 28, 803–806. doi: 10.1029/2000GL012098

Vera, J. D. R., Criado-Aldeanueva, F., García-Lafuente, J., and Soto-Navarro, F. J. (2009). A new insight on the decreasing sea level trend over the Ionian basin in the last decades. *Global Planetary Change* 68, 232–235. doi: 10.1016/j.gloplacha.2009.04.002

Vigo, I., García, D., and Chao, B. F. (2005). Change of sea level trend in Mediterranean and black seas. *J. Mar. Res.* 63, 1085–1100. doi: 10.1357/002224005775247607

Vigo, M. I., Sánchez-Reales, J. M., Trottini, M., and Chao, B. F. (2011). Mediterranean Sea Level variations: Analysis of the satellite altimetric data 1992–2008. *J. Geodynamics* 52, 271–278. doi: 10.1016/j.jog.2011.02.002

Vilibić, I., Matijević, S., Šepić, J., and Kušpilić, G. (2012). Changes in the Adriatic oceanographic properties induced by the Eastern Mediterranean transient. *Biogeosciences* 9, 2085–2097. doi: 10.5194/bg-9-2085-2012

von Schuckmann, K., Le Traon, P. Y., Smith, N., Pascual, A., Djavidnia, S., Gattuso, J. P., et al. (2019). Copernicus Marine service ocean state report. *J. Oper. Oceanogr.* 12 (3), S1–S123. doi: 10.1080/1755876X.2019.1633075

Watson, C. S., White, N. J., Church, J. A., King, M. A., Burgette, R. J., and Legresy, B. (2015). Unabated global mean sea-level rise over the satellite altimeter era. *Nat. Clim. Change* 5, 565–568. doi: 10.1038/nclimate2635

WCRP Global Sea Level Budget Group (2018). Global sea-level budget 1993–present. *Earth Syst. Sci. Data* 10, 1551–1590. doi: 10.5194/essd-10-1551-2018

Winer, B. J. (1962). *Statistical principles in experimental design* (NewYork, NY, US: McGraw-Hill Book Company).

Wöppelmann, G., and Marcos, M. (2012). Coastal sea level rise in southern Europe and the nonclimate contribution of vertical land motion. *J. Geophys. Res.* 117, C01007. doi: 10.1029/2011JC007469

Zunino, P., Schroeder, K., Vargas-Yáñez, M., Gasparini, G. P., Coppola, L., García-Martínez, M. C., et al. (2012). Effects of the Western Mediterranean transition on the resident water masses: Pure warming, pure freshening and pure heaving. *J. Mar. Syst.* 96-96, 15–23. doi: 10.1016/j.jmarsys.2012.01.011